RADYOLOJİ

Editör: Dr.Öğr.Üyesi Zeliha ÇOŞGUN

yaz
yayınları

RADYOLOJİ

Editör

Dr. Öğr. Üyesi Zeliha ÇOŞGUN

yaz yayınları

2024

yaz
yayınları

RADYOLOJİ

Editör: Dr. Öğr. Üyesi Zeliha ÇOŞGUN

E_ISBN 978-625-6104-77-8

Ekim 2024 – Afyonkarahisar

Dizgi/Mizanpaj: YAZ Yayınları

Kapak Tasarım: YAZ Yayınları

YAZ Yayınları. Yayıncı Sertifika No: 73086

M.İhtisas OSB Mah. 4A Cad. No:3/3
İscehisar/AFYONKARAHİSAR

www.yazyayinlari.com

yazyayinlari@gmail.com

info@yazyayinlari.com

İÇİNDEKİLER

RADIOLOGICAL IMAGING METHODS IN LOWER EXTREMITY PERIPHERAL ARTERY DISEASE

Merve BAŞDEMİRCİ[1]

1. INTRODUCTION

Peripheral artery disease (PAD) of the lower extremities is a common and progressive disease that affects the iliac arteries and more distal arteries, often developing due to atherosclerotic changes. Due to atherosclerosis, different degrees of lumen stenosis or occlusion occur in the affected arteries. Its frequency increases with age, and it is reported to be seen in % 3-10 of the population and %15-20 of those over the age of 70 (Fowkes, 1988; Selvin & Erlinger, 2004). In a study carried out in our country, it was determined that the prevalence in the study population was %20 (Bozkurt, Tasci, Tabak, Gumus, & Kaplan, 2011).

It has been reported that the risk of cardiovascular mortality and morbidity is higher and the quality of life decreases in individuals diagnosed with lower extremity peripheral artery disease (LEPAD) (McDermott et al., 2015; Ruo et al., 2007). The fact that the disease affects a wide age range and is associated with increased morbidity/mortality underscores the importance of early diagnosis and treatment.

[1] Radiology Specialist, Karabük Training and Research Hospital, Department of Radiology, gokceoglumrv@gmail.com, ORCID: 0000-0002-8409-9356.

1.1.Risk Factors

Risk factors for LEPAD include smoking, Diabetes Mellitus (DM), hypertension (HT), hyperlipidemia, obesity, advanced age, and family history (Eraso et al., 2014). Smoking is the most significant risk factor affecting the severity of the disease. It has been reported that patients who smoke have a shorter life expectancy and an increased likelihood of critical ischemia and amputation compared to non-smokers (Jelani et al., 2018).

1.2.Clinical Presentation

Depending on the degree of involvement of arterial structures in patients, signs of acute ischemia, critical ischemia, and chronic PAD may be observed. In acute ischemia, due to the sudden interruption of arterial circulation to the limb, patients present with absent pulses, motor weakness in the affected limb, and a cold, painful extremity.

In critical ischemia, there is arterial narrowing that poses a threat to the extremity, and patients may present with leg pain at rest, tissue loss, ischemic ulcer or gangrene. In chronic PAD, symptoms such as leg pain during walking (intermittent claudication), atrophic changes in the legs, weakened pulses, and arterial murmurs may be observed. Although %40 of patients are asymptomatic, the most common symptom is intermittent claudication. Intermittent claudication is characterized by leg pain that arises during physical activity and subsides with rest (Kannel & McGee, 1985; McDermott et al., 2001).

Fontaine (Table 1) and Rutherford (Table 2) classifications are used to clinically classify patients according to their symptoms (Fontaine, Kim, & Kieny, 1954; Rutherford et al., 1997).

Table 1. Fontaine classification

Fontaine classification	
Stage	**Clinical**
I	Asymptomatic
IIA	Claudication at a distance of more than 200m
IIB	Claudication at less than 200m distance
III	Ischemic rest pain
IV	Ulcer, gangrene

Source: (Fontaine et al., 1954)

Table 2. Rutherford classification

Rutherford classification	
Stage	**Clinical**
0	Asymptomatic
1	Mild claudication
2	Moderate claudication
3	Severe claudication
4	Pain at rest
5	Minor tissue loss, ischemic ulcer
6	Major tissue loss, gangrene

Source: (Rutherford et al., 1997)

1.3.Anatomy

To perform an accurate radiological evaluation and reporting, it is essential to have a good grasp of the anatomy of the arterial vascular system.

The external iliac artery is referred to as the main femoral artery from the level of the inguinal ligament, and the main femoral artery branches into the deep femoral artery (DFA) and superficial femoral artery (SFA). DFA has a deep course in the posterolateral aspect. The SFA extends medially to the adductor hiatus and continues as the popliteal artery (PA) after exiting the Hunter canal. The PA branches into two arteries: the anterior tibial artery (ATA) and tibioperoneal trunk (TPT). The ATA travels along the anterior compartment of the leg and continues as the arteria dorsalis pedis (ADP) on the dorsum of the foot. The

TPT is divided into two branches,: the peroneal artery and the posterior tibial artery (ATP), both of which run in the posterior compartment of the leg. The ATP runs behind the medial malleolus and branches into plantar branches.

2. IMAGING METHODS

Different radiological imaging methods are used in the diagnosis of LEPAD. Non-invasive imaging methods include Ultrasonography (US), Computed Tomography (CT) and Magnetic Resonance Imaging (MRI), while Digital Subtraction Angiography (DSA) is used as an invasive imaging method.

Radiologic imaging techniques allow for the assessment of arteries with stenosis or occlusion, the degree of stenosis in the affected artery, vascular flow distal to the stenosis or occlusion, collateral circulation, plaque morphology, and extent. Additionally, this information helps in identifying the appropriate treatment method.

2.1.Non-Invasive Imaging Methods

2.1.1. Ultrasonography (US)

LEPAD, the first preferred imaging method is Ultrasonography (US). Grayscale (B-mode) and Doppler US are used in the examination. The combination of color Doppler ultrasound and B-mode is referred to as duplex ultrasound. With duplex US, in addition to arterial hemodynamics, the location of vascular stenosis, the degree of stenosis, plaque morphology, and its extent can also be assessed (Norgren et al., 2007).

By performing morphological evaluation and plaque characterization in the affected arterial structure using B-mode US, it is possible to assess whether the plaque is calcified or non-calcified, has a smooth or irregular surface, its thickness, how much it surrounds the lumen, and the degree of stenosis.

Doppler ultrasound enables the evaluation of the presence of intraluminal blood flow, flow direction, flow pattern, and peak systolic velocity (PSV). The ratio of PSV between the stenotic area and the adjacent normal vessel is used to assess the degree of narrowing. A PSV of over 200 cm/sec in the stenotic area and/or a PSV ratio exceeding 2 is regarded as significant an indicator of hemodynamically significant stenosis (Allan, 2006; Donnelly, Hinwood, & London, 2000).

A triphasic flow pattern with high resistance should be seen in normal lower extremity arteries (Figure1). However, in cases of ischemia, the collateral circulation and vasodilation that occur distal to the stenosis lead to a decrease in resistance and the development of a biphasic flow pattern. Biphasic flow pattern can be seen in distal lower extremity arteries (ATP, ADP) and should not be considered pathological. However, as stenosis progresses, flow pulsatility diminishes due to vasodilation, resulting in a monophasic flow pattern (Figure 2). Monophasic flow pattern is a pathological finding for all extremity arteries.

Figure 1. B-mode (A) and Color Doppler (B) ultrasound, normal appearance of the common femoral artery (CFA), deep femoral artery (DFA), and superficial femoral artery (SFA) is shown. Spectral Doppler (C) ultrasound image shows the normal triphasic flow pattern observed in the arteries of the lower extremities.

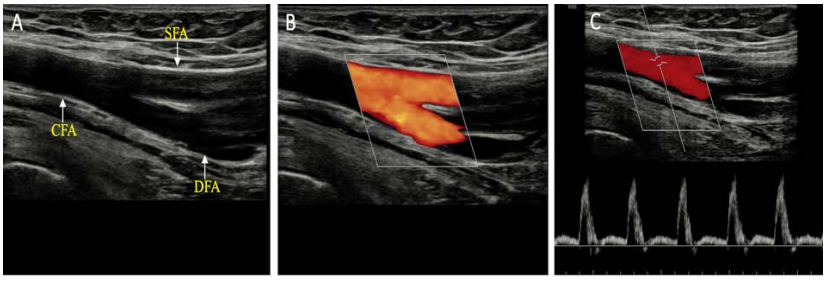

Figure 2. B-mode (A) US image, plaques (asterisks) causing stenosis in the superficial femoral artery (SFA) are observed. In the color Doppler (B) and spectral Doppler (C) US images, color aliasing and a biphasic flow pattern due to stenosis in the SFA are noted. In the transverse view color Doppler (D) and longitudinal view color Doppler (E) US images, occlusion of the anterior tibialis artey (ATA) and twinkle artifact (arrowhead) caused by calcified plaques on the wall are observed. The spectral Doppler US image (F) monophasic flow pattern in the arteria dorsalis pedis (ADP) is observed.

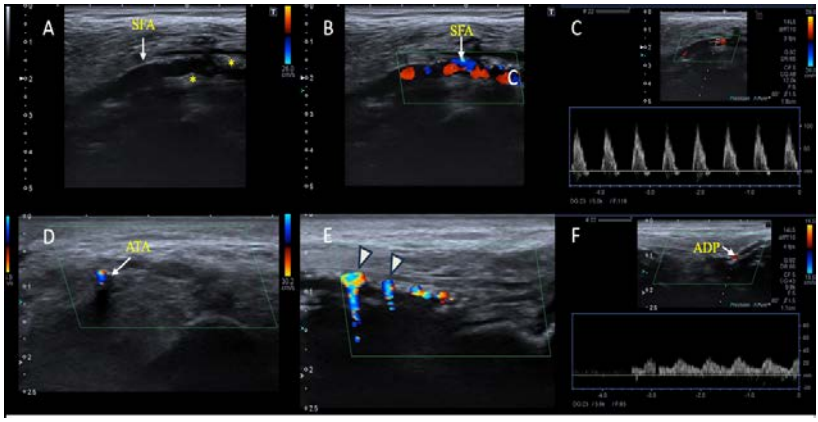

In a patient with acute occlusion, Doppler ultrasound shows the absence of intraluminal blood flow, whereas in patients with critical stenosis, Doppler ultrasound reveals an increase in peak systolic velocity in the stenotic segment, a disruption of laminar flow secondary to the narrowing of the lumen, and the presence of aliasing artifacts at that level (Figure 3,4)

Figure 3: In the transverse, B-mode (A) and color Doppler (B) US images show a plaque that circles the lumen of the right common femoral artery at 180 degrees. The longitudinal color Doppler US image (C) shows a significant decrease in the diameter of the left superficial femoral artery (SFA). The longitudinal B-mode US image (D), transverse color Doppler US image (E), and longitudinal color Doppler US image (F) demonstrate occlusion of the left SFA, while the left deep (DFA) and common femoral arteries (CFA) appear patent.

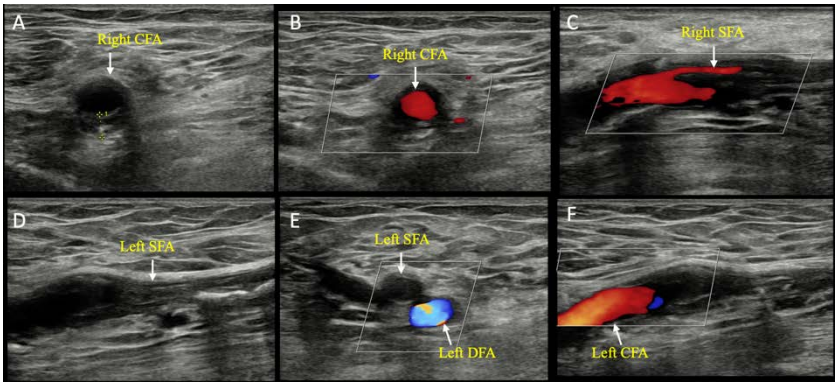

Figure 4. In the B-mode (A) US image, plaques (asterisks) causing stenosis in superficial femoral artery (SFA) are observed, and in color Doppler US image, aliasing artifacts (arrowheads) are shown in the regions of stenosis.

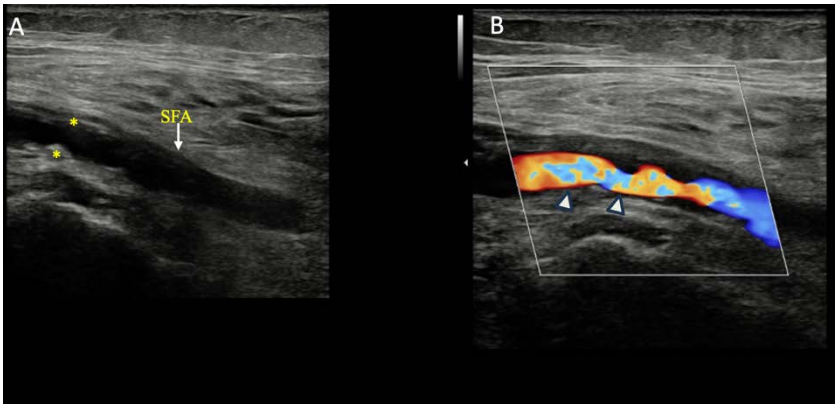

In addition to guiding the diagnosis and treatment selection, US also enables patient follow-up with serial examinations to evaluate the openness of the stent or bypass graft after treatment (Ali F. AbuRahma, 2010) (Figure 5).

Figure 5. B-mode (A), color Doppler (B), and spectral Doppler (C) US images show that the stent placed in the superficial femoral artery (SFA) is patent, with a triphasic flow pattern observed within the stent.

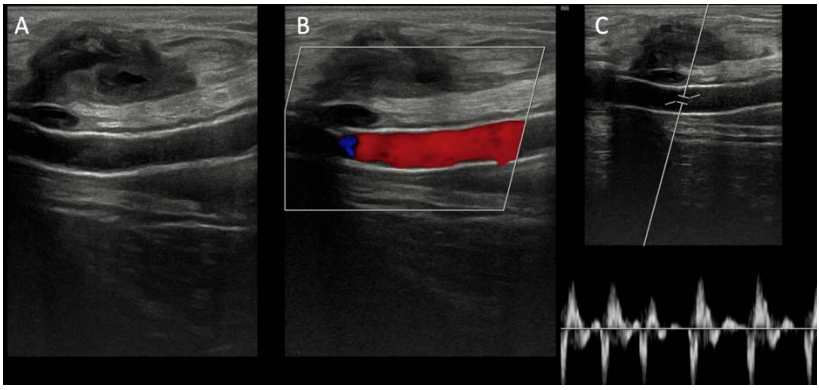

Ultrasound has several advantages, including being non-invasive, cost-effective, repeatable, radiation-free, and allowing for bedside evaluation. The disadvantages include the inability to optimally assess deep areas, the inability to evaluate the entire course of arterial structures, challenges in lumen assessment in obese, edematous, or patients with a high burden of calcific plaques and the operator-dependent of the evaluation.Clinical and physiological characteristics of patients (such as poor general condition or the presence of open wounds or bandages in the examination area) may also make the sonographic examination of arterial structures difficult.

To summarize, duplex ultrasound is an appropriate imaging technique for evaluating stenotic regions, monitoring after treatment, and determining the treatment method (Hwang, 2017). However, some limitations (such as operator dependency

and widespread calcific plaques) create a need for additional imaging.

2.1.2. Computed Tomography Angiography (CTA)

CTA is commonly utilized and easily accessible imaging method that allows for the assessment of the entire vascular system of the lower extremities, starting from the level of the abdominal aorta in a single scan (Zettervall, Marshall, Fleser, & Guzman, 2018). In addition to identifying the location of stenosis, visualizing the entire vascular tract and detecting multifocal stenoses that cannot be seen sonographically are important for treatment planning.

The advantages of CTA include its speed, being a non-invasive method, the ability to evaluate the entire vascular structure, having high resolution, and providing a more objective assessment. However, in addition to its advantages, it also has several disadvantages.

In cases of pre-occlusive stenoses, the failure to detect blood flow may result in incorrect interpretations suggesting an occlusion. In patients with a high burden of calcific plaques (especially in the infrapopliteal region), the beam hardening artifact caused by these plaques may lead to incorrect assessments or no assessment of the extent of stenosis (Figure 6). Additionally, radiation exposure and the use of iodinated contrast agents are among the disadvantages. The use of iodinated contrast agents in imaging may pose limitations for patients with chronic kidney disease or those who have a history of allergic reactions to contrast agents.However, despite all these disadvantages, CTA continues to be one of the most frequently utilized imaging techniques, especially for patients needing treatment planning.

Figure 6. In the axial CTA (A) slices, calcified plaques surrounding the lumen are observed in both superficial and deep femoral arteries. In the coronal MIP (B), 3D volume rendering (C), and 3D MIP (D) images, multifocal stenoses are seen in both SFA, while contrast filling in the distal crural arteries cannot be distinguished. In the sagittal MIP images (E, F), calcified plaques surrounding the lumen in the crural branches are observed and the excessive burden of these calcified plaques makes it challenging to assess lumen patency in some areas.

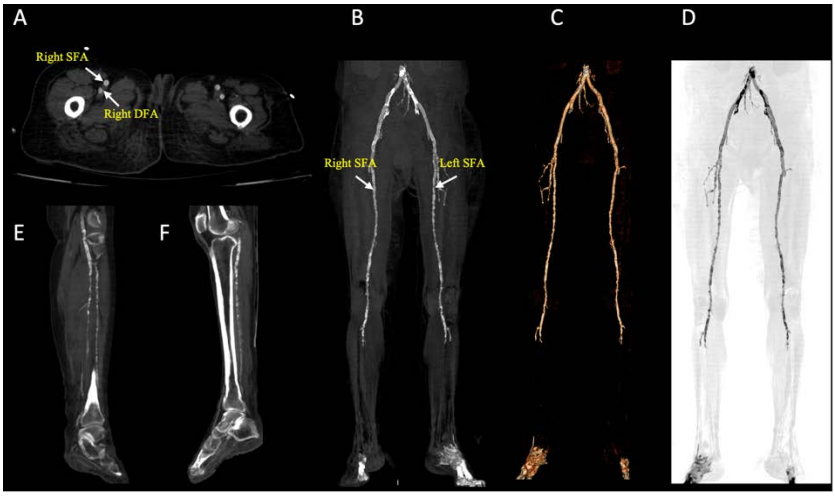

With CTA, the anatomical identification of the region with stenosis/occlusion, calculation of the degree of narrowing, length of the affected segment, whether multifocal stenosis is present, the presence or absence of flow distal to the stenosis, the existence of collateral circulation, the characteristics of the plaque in the stenotic area (such as calcific or non-calcific, how much of the lumen the plaque encircles) can provide guiding information for determining the patient's treatment plan (Figure 7,8).

Figure 7. In the axial CTA slices (A,B), stenosis and occlusion are observed in a short segment of the right superficial femoral artery (SFA). The coronal maximum intensity projection (MIP)(C), 3D volume rendering (D), and 3D MIP (E) images show multifocal stenoses and short segment occlusion in the right SFA, while the crural arteries is patent.

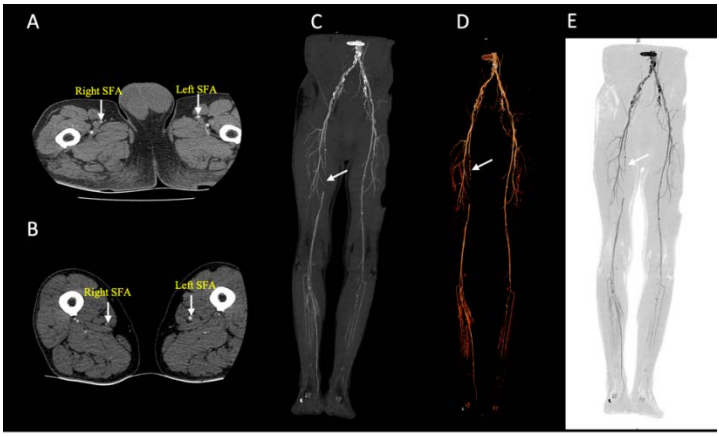

Figure 8. In the coronal 3D MIP (A) and left (B) and right (C) sagittal MIP images, widespread calcified plaques and occlusion are observed in both SFA; there is collateral-dependent contrast filling distal to the occlusion. In the axial CTA slices, both SFA are occluded at the thigh level (D), while at the crural level (E), contrast filling is present in the arteria tibialis anterior (ATA), peroneal artery (PA), and arteria tibialis posterior (ATP).

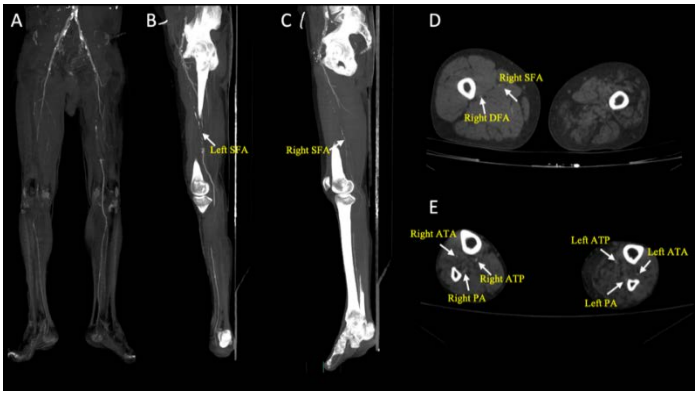

Volume rendering (VR) 3D reconstruction and Maximum Intensity Projection (MIP) images can be obtained from CTA images with post-processing techniques. While VR 3D reconstruction images offer a quick overview for diagnosing pathology, MIP images resemble traditional angiography and assist in assessing the level of stenosis (Pollak, Norton, & Kramer, 2012). Literature indicates that CTA has a sensitivity of %96 and a specificity of %98 for detecting stenoses greater than %50 in the aortoiliac region, while in the femoropopliteal region, it has a sensitivity of %97 and a specificity of %94 (Aboyans et al., 2018; Jens, Koelemay, Reekers, & Bipat, 2013; Met, Bipat, Legemate, Reekers, & Koelemay, 2009).

Although CTA is a helpful imaging method for treatment planning in patients, factors such as significant wall calcification, small vessel diameters, and insufficient contrast attenuation, particularly in infrapopliteal region, can lead to diagnostic challenges. Different techniques can be used to avoid such limitations. Dual energy CT (DECT) is a CT technology that allows for the generation of numerous image datasets by utilizing two different X-ray spectra. It provides more detailed imaging and has been reported to have high sensitivity in detecting stenoses (De Santis et al., 2019; Kosmala et al., 2022). With the dual energy used in DECT, bone can be identified and removed from the obtained images, allowing only the visualization of only the vascular structures that contain contrast material (Sommer et al., 2009). In addition to automatic bone removal, calcific plaques can also be removed from the images, allowing for better assessment of patent lumens in MIP images (Meyer et al., 2008). However, the use of DECT is still limited when compared to conventional single-energy CT.

2.1.3. Magnetic Resonance Angiography (MRA)

Magnetic resonance angiography (MRA) has been report to be a dependable imaging technique for evaluating the presence and severity of stenosis in patients with intermittent claudication and chronic critical ischemia (Iglesias & Peña, 2014; Jens et al., 2013). There are three different MRA sequences for peripheral arterial imaging.

a) Time of Flight Angiography (TOF): It is a technique for visualizing intravascular blood flow based on blood flow, without employing contrast agents. As a result of sections taken perpendicular to the blood flow, gradient differences in protons due to the flow provide images.To achieve a contrast difference between the blood in the vessel and the stationary tissue, the blood flow must be rapid. Regions where blood flow slows down or when the section is taken parallel to the flow may result in signal loss, leading to misinterpretations. Being sensitive to motion and susceptibility artifacts, having a prolonged imaging acquisition time, and experiencing signal loss in areas with turbulent flow are of the disadvantages.

b) Phase Contrast Imaging: In this technique, images are obtained by applying two gradients of equal magnitude but opposite direction, resulting in phase shifts among the protons in the blood. The examination time is longer and more sensitive to artifacts compared to TOF. However, it's not sensitivity to flow velocity allows for better visualization of slow flow compared to TOF. This technique can also provide information about current direction and speed.

c) Contrast-enhanced MRA: Gadolinium-based contrast agents reduce the T1 relaxation time, resulting in hyperintense visualization of intravascular blood. It is a higher resolution and faster MR angiography technique and is less sensitive to motion

and susceptibility artifacts than other MR angiography techniques.

In a comparison of CTA and MRA, MRA can result in misinterpretations as pseudocclusion in regions with low flow velocity and may overestimate the extent of stenosis. Additionally, MRA has several disadvantages, including a longer examination time, sensitivity to motion and susceptibility artifacts, higher costs, and limited accessibility. Incompatibility with a pacemaker or implant in the patient, as well as the presence of metallic objects in the imaging area causing artifacts, are also among the disadvantages. In patients with advanced chronic kidney disease, there is a risk of nephrogenic systemic fibrosis linked to the use of gadolinium-based contrast agents (Ramalho et al., 2016). The advantages of MRA are that it does has high soft tissue resolution, not contain ionizing radiation and does not utilize iodinated contrast agents.

Although MRI sequences have limitations in assessing calcific plaques, the 'black-blood' spin echo sequence can reduce the blood signal within the vessel,for imaging the vessel wall, plaques, and plaque morphology (Mihai et al., 2009). Research has demonstrated that MRI characteristics of plaques can identify individuals at greater risk of endovascular failure (such as difficult to pass with a guidewire) (Roy, Chen, Dueck, & Wright, 2018).

2.2.Invasive Imaging Methods

2.2.1. Digital Subtraction Angiography (DSA)

DSA is the gold standard imaging method for the diagnosis of LEPAD. Besides evaluating lumen patency, stenosis severity, and collateral flow, it also holds significant importance in endovascular treatment. DSA allows for real-time imaging with high contrast resolution using lower doses of IV contrast, while also providing the opportunity for simultaneous treatment (

Figure 9,10). Considering the limitations of other imaging methods in evaluating pre-occlusive stenoses and small-diameter arteries like distal pedal or crural arteries, DSA provides more comprehensive information (Aboyans et al., 2018).

The advantages of DSA include its high-resolution, fast imaging method and provide an opportunity treatment. The disadvantages include being an invasive imaging method, radiation exposure, the inability to visualize the vessel wall, sensitivity to motion artifacts, the use of iodinated contrast agents, and the potential for complications related to arterial puncture during the procedure.

Figure 9. In the digital subtraction angiography (DSA) images, an occlusion in the popliteal artery (A) is observed. After balloon angioplasty (B), the patency of the popliteal artery at the occluded segment is observed.

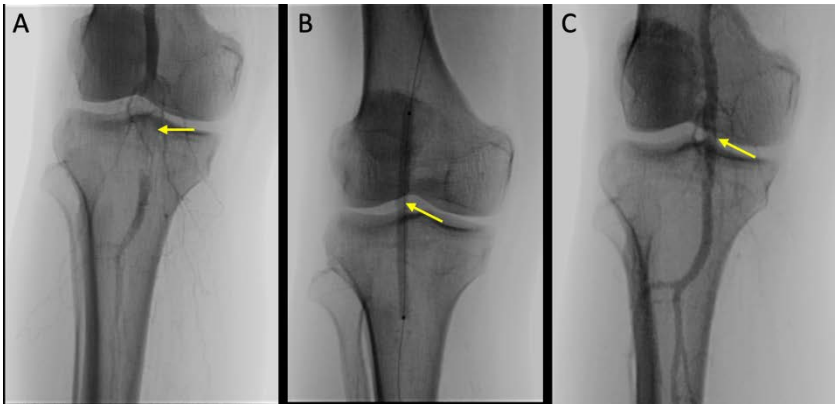

Figure 10. In the coronal subtraction MRA (A), 3D MIP (B), and DSA (C) images, severe stenosis is observed in the left superficial femoral artery (SFA). Following angioplasty, the DSA image (D) demostrate improvement in arterial patency.

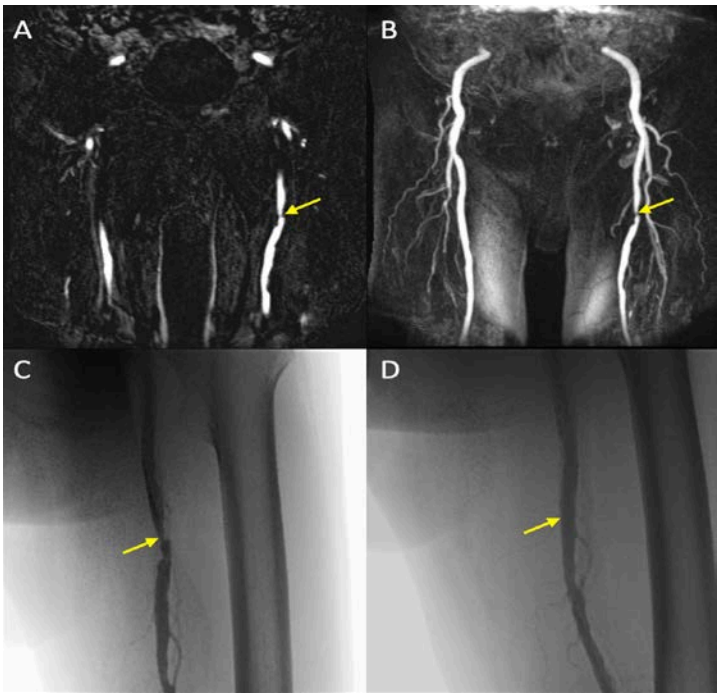

3. CONCLUSION

In diagnosing LEPAD and planning treatment strategies, the choice of imaging techniques should be customized for each patient, considering their symptoms, comorbidities, and overall health status. Choosing a suitable imaging method, understanding the limitations of the selected technique, and, when necessary, using a combination of different imaging modalities will aid in evaluating the extent of the disease and planning an appropriate treatment plan.

REFERENCES

Aboyans, V., Ricco, J. B., Bartelink, M. E. L., Björck, M., Brodmann, M., Cohnert, T., . . . Desormais, I. (2018). 2017 ESC Guidelines on the Diagnosis and Treatment of Peripheral Arterial Diseases, in collaboration with the European Society for Vascular Surgery (ESVS): Document covering atherosclerotic disease of extracranial carotid and vertebral, mesenteric, renal, upper and lower extremity arteriesEndorsed by: the European Stroke Organization (ESO)The Task Force for the Diagnosis and Treatment of Peripheral Arterial Diseases of the European Society of Cardiology (ESC) and of the European Society for Vascular Surgery (ESVS). Eur Heart J, 39(9), 763-816. doi:10.1093/eurheartj/ehx095

Ali F. AbuRahma, J. J. B. (2010). Noninvasive Peripheral Arterial Diagnosis: Springer London.

Allan, P. L. P. (2006). Clinical Doppler ultrasound. In. Retrieved from http://www.clinicalkey.com/dura/browse/bookChapter/3-s2.0-C2009059900X

Bozkurt, A. K., Tasci, I., Tabak, O., Gumus, M., & Kaplan, Y. (2011). Peripheral artery disease assessed by ankle-brachial index in patients with established cardiovascular disease or at least one risk factor for atherothrombosis--CAREFUL study: a national, multi-center, cross-sectional observational study. BMC Cardiovasc Disord, 11, 4. doi:10.1186/1471-2261-11-4

De Santis, D., De Cecco, C. N., Schoepf, U. J., Nance, J. W., Yamada, R. T., Thomas, B. A., . . . Albrecht, M. H. (2019). Modified calcium subtraction in dual-energy CT angiography of the lower extremity runoff: impact on

diagnostic accuracy for stenosis detection. Eur Radiol, 29(9), 4783-4793. doi:10.1007/s00330-019-06032-y

Donnelly, R., Hinwood, D., & London, N. J. (2000). ABC of arterial and venous disease. Non-invasive methods of arterial and venous assessment. BMJ, 320(7236), 698-701. doi:10.1136/bmj.320.7236.698

Eraso, L. H., Fukaya, E., Mohler, E. R., 3rd, Xie, D., Sha, D., & Berger, J. S. (2014). Peripheral arterial disease, prevalence and cumulative risk factor profile analysis. Eur J Prev Cardiol, 21(6), 704-711. doi:10.1177/2047487312452968

Fontaine, R., Kim, M., & Kieny, R. (1954). [Surgical treatment of peripheral circulation disorders]. Helv Chir Acta, 21(5-6), 499-533.

Fowkes, F. G. (1988). Epidemiology of atherosclerotic arterial disease in the lower limbs. Eur J Vasc Surg, 2(5), 283-291. doi:10.1016/s0950-821x(88)80002-1

Hwang, J. Y. (2017). Doppler ultrasonography of the lower extremity arteries: anatomy and scanning guidelines. Ultrasonography, 36(2), 111-119. doi:10.14366/usg.16054

Iglesias, J., & Peña, C. (2014). Computed tomography angiography and magnetic resonance angiography imaging in critical limb ischemia: an overview. Tech Vasc Interv Radiol, 17(3), 147-154. doi:10.1053/j.tvir.2014.08.003

Jelani, Q. U., Petrov, M., Martinez, S. C., Holmvang, L., Al-Shaibi, K., & Alasnag, M. (2018). Peripheral Arterial Disease in Women: an Overview of Risk Factor Profile, Clinical Features, and Outcomes. Curr Atheroscler Rep, 20(8), 40. doi:10.1007/s11883-018-0742-x

Jens, S., Koelemay, M. J., Reekers, J. A., & Bipat, S. (2013). Diagnostic performance of computed tomography angiography and contrast-enhanced magnetic resonance angiography in patients with critical limb ischaemia and intermittent claudication: systematic review and meta-analysis. Eur Radiol, 23(11), 3104-3114. doi:10.1007/s00330-013-2933-8

Kannel, W. B., & McGee, D. L. (1985). Update on some epidemiologic features of intermittent claudication: the Framingham Study. J Am Geriatr Soc, 33(1), 13-18. doi:10.1111/j.1532-5415.1985.tb02853.x

Kosmala, A., Weng, A. M., Schmid, A., Gruschwitz, P., Grunz, J. P., Bley, T. A., & Petritsch, B. (2022). Dual-Energy CT Angiography in Peripheral Arterial Occlusive Disease: Diagnostic Accuracy of Different Image Reconstruction Approaches. Acad Radiol, 29 Suppl 4, S59-s68. doi:10.1016/j.acra.2020.10.028

McDermott, M. M., Guralnik, J. M., Criqui, M. H., Ferrucci, L., Liu, K., Spring, B., . . . Rejeski, W. J. (2015). Unsupervised exercise and mobility loss in peripheral artery disease: a randomized controlled trial. J Am Heart Assoc, 4(5). doi:10.1161/jaha.114.001659

McDermott, M. M., Kerwin, D. R., Liu, K., Martin, G. J., O'Brien, E., Kaplan, H., & Greenland, P. (2001). Prevalence and significance of unrecognized lower extremity peripheral arterial disease in general medicine practice*. J Gen Intern Med, 16(6), 384-390. doi:10.1046/j.1525-1497.2001.016006384.x

Met, R., Bipat, S., Legemate, D. A., Reekers, J. A., & Koelemay, M. J. (2009). Diagnostic performance of computed tomography angiography in peripheral arterial disease: a

systematic review and meta-analysis. Jama, 301(4), 415-424. doi:10.1001/jama.301.4.415

Meyer, B. C., Werncke, T., Hopfenmüller, W., Raatschen, H. J., Wolf, K. J., & Albrecht, T. (2008). Dual energy CT of peripheral arteries: effect of automatic bone and plaque removal on image quality and grading of stenoses. Eur J Radiol, 68(3), 414-422. doi:10.1016/j.ejrad.2008.09.016

Mihai, G., Chung, Y. C., Kariisa, M., Raman, S. V., Simonetti, O. P., & Rajagopalan, S. (2009). Initial feasibility of a multi-station high resolution three-dimensional dark blood angiography protocol for the assessment of peripheral arterial disease. J Magn Reson Imaging, 30(4), 785-793. doi:10.1002/jmri.21923

Norgren, L., Hiatt, W. R., Dormandy, J. A., Nehler, M. R., Harris, K. A., & Fowkes, F. G. (2007). Inter-Society Consensus for the Management of Peripheral Arterial Disease (TASC II). J Vasc Surg, 45 Suppl S, S5-67. doi:10.1016/j.jvs.2006.12.037

Pollak, A. W., Norton, P. T., & Kramer, C. M. (2012). Multimodality imaging of lower extremity peripheral arterial disease: current role and future directions. Circ Cardiovasc Imaging, 5(6), 797-807. doi:10.1161/circimaging.111.970814

Ramalho, J., Semelka, R. C., Ramalho, M., Nunes, R. H., AlObaidy, M., & Castillo, M. (2016). Gadolinium-Based Contrast Agent Accumulation and Toxicity: An Update. AJNR Am J Neuroradiol, 37(7), 1192-1198. doi:10.3174/ajnr.A4615

Roy, T. L., Chen, H. J., Dueck, A. D., & Wright, G. A. (2018). Magnetic resonance imaging characteristics of lesions relate to the difficulty of peripheral arterial endovascular

procedures. J Vasc Surg, 67(6), 1844-1854.e1842. doi:10.1016/j.jvs.2017.09.034

Ruo, B., Liu, K., Tian, L., Tan, J., Ferrucci, L., Guralnik, J. M., & McDermott, M. M. (2007). Persistent depressive symptoms and functional decline among patients with peripheral arterial disease. Psychosom Med, 69(5), 415-424. doi:10.1097/PSY.0b013e318063ef5c

Rutherford, R. B., Baker, J. D., Ernst, C., Johnston, K. W., Porter, J. M., Ahn, S., & Jones, D. N. (1997). Recommended standards for reports dealing with lower extremity ischemia: revised version. J Vasc Surg, 26(3), 517-538. doi:10.1016/s0741-5214(97)70045-4

Selvin, E., & Erlinger, T. P. (2004). Prevalence of and risk factors for peripheral arterial disease in the United States: results from the National Health and Nutrition Examination Survey, 1999-2000. Circulation, 110(6), 738-743. doi:10.1161/01.Cir.0000137913.26087.F0

Sommer, W. H., Johnson, T. R., Becker, C. R., Arnoldi, E., Kramer, H., Reiser, M. F., & Nikolaou, K. (2009). The value of dual-energy bone removal in maximum intensity projections of lower extremity computed tomography angiography. Invest Radiol, 44(5), 285-292. doi:10.1097/RLI.0b013e31819b70ba

Zettervall, S. L., Marshall, A. P., Fleser, P., & Guzman, R. J. (2018). Association of arterial calcification with chronic limb ischemia in patients with peripheral artery disease. J Vasc Surg, 67(2), 507-513. doi:10.1016/j.jvs.2017.06.086

OTOSKLEROZ VE RADYOLOJİK DEĞERLENDİRMESİ

Hanife Gülden DÜZKALIR[1]

1. GİRİŞ

Bu bölüm, otosklerozun klinik bulguları ile radyoloji pratiğindeki tipik ve atipik özelliklerini vurgulayarak entegre bir şekilde okuyucunun bu hastalığı etkili bir şekilde teşhis etme ve tedaviyi yönetme becerisini arttırabilmeyi hedeflemektedir.

1.1.Otoskleroza Genel Bakış

Otoskleroz ağırlıklı olarak stapes ve kokleayı çevreleyen kemik labirenti etkileyen, otik kapsül kemik rezorpsiyonu, yeni kemik birikimi ve vasküler proliferasyonu da içeren anormal temporal kemik remodelingi ile karakterize patolojik bir durumdur. Otoskleroz patogenezinde otik kapsüldeki fokal dejenerasyon otik kapsülde bulunan benzersiz kemik ortamıyla ilişkilendirilebilir. Doğumdan sonra iç kulak çevresinde normal kemik remodelingi neredeyse yoktur. Bu da dejeneratif değişikliklerin ve ölü osteositlerin birikmesine neden olur. Bundan yüksek düzeyde iç kulak anti rezorptif osteoprotegerin sorumludur. İnsan otik kapsülündeki otosklerotik tercih bölgelerinde, hücresel boşluklar olarak adlandırılan, ara sıra ölü osteosit kümeleri oluştuğu gösterilmiştir. Bu hücresel boşluklar da otosklerozun olası başlangıç noktaları olarak öne sürülmüştür. İnaktif otosklerotik lezyonlar genelde ölü interstisyel kemikten oluşur (Hansen ve ark., 2023; Vîrzob ve ark., 2023).

[1] Uzman Dr., Sağlık Bilimleri Üniversitesi, Kartal Dr. Lütfi Kırdar Şehir Hastanesi, Radyoloji Bölümü, hanifeduzkalir@gmail.com, ORCID: 0000-0002-3514-8158.

Otoskleroz en sık tek taraflı iletim tipi işitme kaybıyla ortaya çıksa da mikst işitme kaybı şeklinde de ortaya çıkabilir (Foster ve ark., 2023). Anormal remodeling özellikle otik kapsülde stapes foot plate çevresindedir. Hastalık idiyopatik ve ilerleyicidir. Stapedial fiksasyona yol açarak ses titreşimlerinin iç kulağa iletilmesini bozması sonucunda iletim tipi işitme kaybı ortaya çıkar. Otosklerozun bu olgularda kontrollere kıyasla koklear akuaduktun daha dar, daha uzun ve daha fazla huni genişliğine sahip olmasına neden olduğu da bildirilmiştir (Wichova ve ark., 2019). Hastalık ilerleyerek otoskleroz koklear endosteuma yayıldığında, spiral ligaman boyunca kollajen birikmesi ve hair cell işlev bozukluğuyla sensörinöral işitme kaybı gelişebilir (Quesnel ve ark., 2018).

Otoskleroz, beyaz yetişkinler arasında %0.2-1 oranında görülmekte olup, kemikçik zincir hareketliliğinde bozulmaya ve iletim tipi işitme kaybına yol açan bu durumun otik kapsülün anormal kemik homeostazından kaynaklandığı belirtilmektedir (Chen ve ark., 2002). Ancak otosklerozun etiyolojisi tam olarak anlaşılamamıştır ve tedavi seçenekleri sınırlıdır (Rämö ve ark., 2020). Etiyolojide hem genetik hem de çevresel bileşenlerin etkili olduğu düşünülmektedir. Son çalışmalar yeni genetik faktörleri ve potansiyel aday genleri tanımlamaktadır. Hastaların yaklaşık %40'ında hastalık ailesel bir formda mevcuttur (Crompton ve ark., 2019). Hastalığın ailesel kümelenmesi ile genetik faktörler düşünülmektedir. Bu ailelerin çoğunda, otoskleroz az sayıda genetik faktörden (oligojenik) kaynaklanıyor gibi görünürken, sadece az sayıda ailede hastalık gerçekten monojenik gibi görünmektedir (Tavernier ve ark., 2021). Bununla ilgili olarak kemiğin önemli bileşenlerinden biri olan tip I kolajeni kodlayan *COL1A1* genindeki mutasyonlar gibi potansiyel genetik lokuslar ve ilişkileri literatürde tanımlamıştır (McKenna ve ark, 1998). *Forkhead Box L1*'deki (*FOXL1*) patojenik bir delesyonun otozomal dominant otoskleroza neden olduğu ve non-invaziv

terapötik müdahaleler için potansiyel hedefler sağlayabileceği bildirilmiştir (Abdelfatah ve ark., 2021). *RELN* genindeki nadir varyasyon *rs74503667* ve yaygın polimorfizm *rs3914132* ve azalmış ekspresyonlar da otoskleroz ile ilişkilendirilmiştir (Priyadarshi ve ark., 2022). Literatürde otosklerozun genetik olarak boy ve kırık riskiyle ilişkili olduğu ve ilişki lokusların ciddi iskelet bozukluklarıyla örtüştüğü ve *TGF{beta}1* sinyalininin öneminin vurgulandığı çalışma da mevcuttur (Rämö ve ark., 2020). Yine bir başka çalışmada *SMARCA4*'teki bir varyantın, insan otosklerozuna neden olarak, transgenik farelerde benzer etkilerle, işitme bozukluğuna ve otik kapsülde anormal kemik oluşumuna yol açığı belirtilmiştir (Drabkin ve ark., 2023). Bunların yanında çevresel faktörler olarak viral enfeksiyonlar ve florür maruziyetinin de etiyolojide olabileceği bildirilmiştir. Hamilelik sırasında genelde ilerleme görüldüğünden, hormonal faktörlerin de etyolojide yer alabileceği belirtilmiştir (Crompton ve ark., 2019).

Otoskleroz, genellikle mikst işitme kaybının eşlik ettiği iletim tipi işitme kaybı ile kendini gösteren nadir bir hastalıktır. Olgular öykü, fizik muayene ve odyometrik testlerin bir kombinasyonu ile değerlendirilir (Foster ve ark., 2018).

2. KLİNİK BULGULAR

2.1. Klinik Değerlendirme ve Fizik Muayene

Klinik olarak otoskleroz tipik olarak genç yetişkinlerde görülür. Temporal kemiklerde histolojik otoskleroz prevalansı %2.5'tir ve bu oran otosklerotik ailelerde %0.30 ila %0.38 klinik prevalans ile korelasyon göstermektedir (Declau ve ark., 2001). Prevelansı 100.000'de 15-30 bildirilen çalışma mevcuttur (Venurkar ve ark., 2021). Muhtemelen hastalık sürecini hızlandırabilen hamilelik gibi hormonal faktörlerden etkilenmesiyle kadınlarda (%65) erkeklerden (%35) daha

yaygındır (Crompton ve ark., 2019). Tanıda kapsamlı bir klinik öykü ile başlamak önemlidir. Otoskleroz, öncelikle işitsel fonksiyonu etkileyen spesifik klinik belirtilerle karakterizedir. Birincil semptom giderek kötüleşen işitme kaybıdır ve vakaların yaklaşık %80'inde her iki kulağı da etkiler. Tinnitus veya kulak çınlaması da görülebilir. Otosklerozun başlıca klinik belirtileri şu şekilde sıralanabilir:

- ***İlerleyici İleti Tipi İşitme Kaybı:*** Otosklerozun en yaygın ve önemli belirtisidir. Başlangıçta düşük frekansları etkilerken ilerledikçe tüm frekanslara kademeli olarak yayılır. İşitme kaybının sebesi stapes kemiğinin fiksasyonuyla ses titreşimlerini iç kulağa iletme kabiliyetinin azalmasıdır (Zafar ve ark, 2024).
- ***Tinnitus:*** Otoskleroz olgularında sıklıkla (%62) kulaklarda kalıcı bir çınlama veya uğultu bildirilmektedir (Anas ve ark., 2023). Şiddeti değişken olup işitme kaybı ilerledikçe daha belirgin hale gelmektedir.
- ***Paracusis Willisii:*** Otosklerozlu bireylerin ilginç bir özelliği olan bu durum gürültülü ortamlarda daha iyi duyabilmelerini tanımlar. Bunda fikse stapesin daha yüksek sesler tarafından daha etkili bir şekilde hareket ettirilmesi veya gürültüde işlevi artan diğer orta kulak kaslarının etkisi olabilir (de Wit ve van Dishoeck, 1964).
- ***Schwartz İşareti:*** Timpanik membrandan görülen promontoriumda kırmızımsı veya pembemsi bir kızarıklık ile karakterize olan otoskopik muayene bulgusudur. Bu işaret, aktif otosklerotik lezyonlarla ilişkili vasküler anomalilerin göstergesi olarak otosklerozun klasik ancak evrensel olmayan bir göstergesi kabul edilir. Ancak bu işaret her zaman mevcut değildir (House ve Cunningham, 2010; Salomone ve ark., 2008).

Bu klinik belirtiler, otosklerozun tanı ve tedavisinin önemli bir parçasıdır ve diğer işitme kaybı nedenlerinden ayırt edilmesinde yardımcıdır. Literatürde otosklerozun sensörinöral işitme kaybı ve rotatuar vertigo ile ilişkisi bildirilmiş, ancak kan-labirent bariyer bozukluğu ve endolenfatik hidrops gibi MRG bulgularının bu klinik belirtilerle önemli ölçüde ilişkili olmadığı belirtilmiştir (Laine ve ark., 2020).

2.2. Odyometrik Testler

Odyometrik testler otoskleroz teşhisinde oldukça önemli yere sahiptir.

- ***Saf Ton Odyometri:*** İletim tipi bir işitme kaybı mevcuttur. Testte tipik olarak hastalığın erken evrelerinde kemik iletim eşiklerinin hava iletim eşiklerinden daha iyi olduğu görülür. Hastalık ilerledikçe, kokleanın tutulumuna bağlı olarak mikst tip, hatta sensörinöral bileşenli bir işitme kaybı ortaya çıkabilir (Zafar ve ark, 2024; Doherty ve Linthicum, 2004; Merchant ve Rosowski, 2008).
- ***Timpanometri:*** Bu test ise normal orta kulak basınçlarını ve hacimlerini gösterebilir, ayrıca otosklerozun karakteristik işaretlerinden biri olan stapedial refleksin yokluğu veya azalması tespit edilebilir (Zafar ve ark, 2024; Doherty ve Linthicum, 2004; Merchant ve Rosowski, 2008).

3. GÖRÜNTÜLEME

3.1.Tanıda Görüntülemenin Önemi

Otoskleroz tanısında görüntüleme, tanının doğrulanmasına, gereksiz orta kulak incelemelerinin önlenmesine ve orta kulaktaki protez pozisyonunun belirlenmesine yardımcı olur (Wolfovitz ve Luntz; 2018).

Otosklerozda radyolojik değerlendirmenin önemi ve birincil hedefleri şunlardır:

- ***Teşhisin Doğrulanması:*** Otosklerozun benzer şekilde iletim tipi işitme kaybı yapan diğer nedenlerden ayırt edilmesi. Bunda yüksek rezolüsyonlu bilgisayarlı tomografi (HRCT)'de otik kapsüldeki, özellikle oval pencere ve koklea çevresindeki karakteristik kemik değişikliklerinin tanımlanması fayda sağlar.
- ***Hastalık Evrelemesi:*** Görüntüleme, otik kapsülün otospongiotik ve otosklerotik lezyonlarca ne kadar kapsamlı bir şekilde tutulduğunun ve hastalığın fenestral (esas olarak stapes ve oval pencereyi etkileyen) veya retrofenestral (koklea ve bazen iç işitme kanalını içeren) olup olmadığının değerlendirilmesine olanak tanır. Bu ayrım, tedavi seçeneklerini ve prognozu etkilediği için önemlidir.
- ***Cerrahi Planlama:*** Tedavi seçeneklerinden olan stapedektomi veya diğer cerrahi tedaviler için karar verme sürecinde görüntüleme, anatomi ve cerrahi yaklaşımı veya sonucu etkileyebilecek herhangi bir varyasyon veya ek patolojiye ilişkin temel ayrıntılar sağlayarak klinisyene yardımcı olur. Özellikle fasiyal sinirin konumunu ve durumunu, kemikçik zincirinin bütünlüğünü, oval ve yuvarlak pencerelerin durumunu görüntülemede değerlendirme önemlidir.
- ***Diğer Patolojilerin Dışlanması:*** Ayırıcı tanıda yer alan ve otosklerozu taklit edebilen superior semisirküler kanal dehissansı, kemikçik zincir anomalileri veya iç kulak malformasyonları gibi diğer olası işitme kaybı nedenlerinin ekarte edilmesine yardımcı olur.

Bu kısımda otosklerozda radyolojik değerlendirmelerin ayrıntılı hedefleri ve bu rahatsızlığı olan hastalar için genel tanı ve tedavi sürecindeki önemi vurgulanarak özet bilgiler halinde aktarılmaya çalışılmıştır.

3.2.Görüntüleme Teknikleri

3.2.1. Temporal Kemik Yüksek Çözünürlüklü Bilgisayarlı Tomografisi

Otosklerozda temel görüntüleme yöntemi olan Bilgisayarlı Tomografi (BT), mükemmel uzaysal çözünürlüğü nedeniyle otik kapsülün ayrıntılı değerlendirilmesine olanak tanır. Otosklerozun değerlendirilmesinde HRCT tercih edilir. Tipik olarak ince (0.5 ila 1 mm) kesitlerle gerçekleştirilir. Böylece standart BT taramaları ile tespit edilemeyebilecek otosklerozun karakteristik ince kemik değişikliklerinin tanımlanmasına yardımcı olur. Optimum görüntüleme tekniği ve yeterli radyolojik deneyim, vakaların büyük bir kısmında otosklerozu doğru bir şekilde teşhis edebilir ve stapedotomi sonrası komplikasyonların tedavisine yardımcı olur (Kösling ve ark., 2020). Burada dikkat edilmesi gereken önemli noktalar şunlardır:

- Aksiyel ve Koronal Düzlemler: Stapes foot plate ve koklear kapsülü yeterince görüntülemek için görüntüler mutlaka her iki düzlemde de elde edilmelidir. Aksiyel kesitler stapes foot plate ve yuvarlak pencereyi değerlendirmek için çok önemlidir, koronal kesitler ise oval pencereyi ve fasiyal sinirin seyrini daha iyi gösterir.

3.2.1.1.Otoskleroz BT Görüntüleme Bulguları ve Tipleri:

- HRCT'de otoskleroz tipik bulgularından aktif otospongiotik odakları temsil eden hipodens alanlar ve otosklerotik odakları gösteren hiperdens alanlar görülebilir.
- Otosklerozda görülen en yaygın radyolojik özellikler yüzey fissürü (%65), kıkırdak erozyonu (%49) ve osteokondral

arayüzdeki düzensizliktir (%51). Otoskleroz, stapez başının hafif osteoartritine neden olabilir (Clarke-Brodber ve Taxy, 2021).

- Otosklerozdaki "*Çift Halka*" işareti, HRCT'de oval pencerenin daha yoğun bir merkezi kısmını çevreleyen hipodens bir kemik kenarı şeklinde görülür.
- Otosklerozlu hastaların oval pencereye bitişik kemiğinin, normal işiten kişilerden önemli ölçüde daha kalın olduğu, BT'de otik kapsül kalınlığının >2.3 mm olmasının otoskleroz için %96.2 duyarlılığa, %100 özgüllüğe, %100 pozitif öngörü değerine ve %96.4 negatif öngörü değerine sahip olduğu belirtilmiştir (Sanghan vw ark, 2018).
- Hiperostoz: Aşırı kemik oluşumu bazen kokleadan internal akustik kanala doğru uzanım görülebilir.

Tipleri:

- *Fenestral (Stapedial) Otoskleroz*: En yaygın formdur. Stapes ve oval pencere nişini içerir ve genellikle iletim tipi işitme kaybına neden olur. Oval pencerenin bitişiğindeki fissula ante fenestramda kemikte kalınlaşma veya bulanıklaşma BT taramalarında, oval pencerenin anteriorunda fokal bir hipodensite alanı (düşük kemik yoğunluğu) veya berrak lezyon olarak görülür. Bazen lezyon stapes foot plate kalınlaşmasına veya düzensiz bir görünüme neden olabilir. Fissula ante fenestramın (FAF) yüksek çözünürlüklü bilgisayarlı tomografideki yoğunluğunun otoskleroz tanısı için güvenilir bir ölçüm olduğu ve 1.871 HU'dan düşük değerlerin Avrupa Kafkas popülasyonunda en yüksek hassasiyet ve özgüllüğü sergilediği bildirilmiştir (Puiggrós ve ark., 2023).
    - *Tip A:* Fissula ante fenestraya izole, oval pencereyi içeren ve tipik olarak stapes

fiksasyonuna bağlı iletim tipi işitme kaybına neden olur.

o *Tip B:* Stapes foot plate anüler ligamentini içerecek şekilde uzanır, ancak kokleayı etkilemez.

- *Retrofenestral (Koklear) Otoskleroz:* Bu tip, stapesin ötesindeki kemiği, özellikle de kokleayı etkiler. Koklear kapsülü etkilediğinden koklea çevresinde, özellikle yuvarlak pencere düzeyinde demineralizasyon ve kemikte değişiklikler olarak görülebilir. Kokleaya uzanımla hem kemik hem de duyusal yapıları etkileyerek potansiyel olarak mikst veya tamamen sensörinöral işitme kaybına neden olabilir.

  o *Tip C:* Oval pencerenin bütünlüğünü etkilemeden koklear otik kapsülü içerir. Bu tip genellikle hem iletim hem de sensörinöral defisit unsurlarını birleştiren karışık bir işitme kaybına yol açar.

  o *Tip D:* Kokleanın internal akustik kanalına doğru uzanabilen geniş tutulumu, tipik olarak sensörinöral ağırlıklı işitme kaybıyla sonuçlanır.

- *Global Otoskleroz (Diffüz tutulum):* Daha ciddi vakalarda, otoskleroz hem fenestral hem de retrofenestral bölgeleri yaygın olarak tutabilir ve yukarıdaki belirtilerin bir kombinasyonunun yanı sıra iç işitme kanalını veya temporal kemiğin diğer kısımlarını içerebilecek ek tutulum gösterebilir.

  o Tip E: Hem fenestral hem de retrofenestral tiplerin özelliklerini gösterir, stapes foot plate,

oval pencere ve koklear otik kapsülü etkiler ve genellikle mikst tipte önemli işitme kaybına yol açar.

Derecelendirme:

Symons/Fanning derecelendirme sistemine göre otoskleroz olguları şu şekilde sınıflandırılmıştır (Marshall AH ve ark., 2005):

- Derece 1: yalnızca fenestral;
- Derece 2: bazal koklear dönüşe (derece 2A) veya orta/apikal dönüşlere (derece 2B) veya hem bazal dönüşe hem de orta/apikal dönüşlere (derece 2C) doğru yamalı lokalize koklear hastalık (fenestral tutulum olsun ya da olmasın);
- Derece 3: yaygın birleşik koklear tutulum (fenestral tutulum olsun ya da olmasın).

Bu çalışmada derece 3 hastalığı olan otosklerotiklerde önemli bir fasiyal sinir stimülasyon riski varlığı da bildirilmiştir.

- Erken evre otosklerozda radyolojik olarak belirsiz lezyonlar gizli olabilir, bu durum görüntülemede karşılaşılan zorluklardandır. Yüksek çözünürlüklü görüntüleme ve deneyimli bir radyolojik yorumlama gerektirir.

Bu kısımda özellikle YRBT yoluyla yapılan radyolojik değerlendirme ile tespit edilen farklı bulguların otosklerozun tanı ve yönetimi için ne kadar önemli olduğunu ve hastalığın ilerleyişi ve kapsamı hakkında ayrıntılı bilgiler sağladığını, otosklerozun sınıflandırılmasında nasıl önemli bir rol oynadığını, hastalığın işitsel sistem üzerindeki etkisinin anlaşılmasını kolaylaştırdığını ve tedavi yaklaşımına rehberlik ettiğini vurgulayan literatür verilerinden özet bilgiler aktarılmaya çalışılmıştır (Valvassori, 1993; Mafee ve ark., 2004; Naumann ve ark., 2005).

3.2.2. Manyetik Rezonans Görüntüleme

Bilgisayarlı tomografi otoskleroz için, özellikle kemik detaylarını görüntülemek için birincil görüntüleme yöntemi olmakla birlikte, Manyetik Rezonans Görüntüleme (MRG) özellikle ileri evrelerde veya koklear implantasyon gibi tedavi kararlarını etkileyebilecek koklear tutulumu değerlendirmede önemli rol oynar. MRG postoperatif komplikasyonların değerlendirilmesinde ve aktif osteosklerozun tedavisinde sınırlı ancak önemli endikasyonlara sahiptir (Mangia ve ark., 2020). Otoskleroz olduğundan şüphelenilen hastalarda temporal kemiklerin MRG'si tipik olarak şunları içermelidir:

- Yüksek çözünürlüklü T1 ağırlıklı ve T2 ağırlıklı görüntüler: Bu sekanslar iç kulak ve koklea çevresindeki yumuşak doku yapılarını görüntülemek için faydalıdır.
- Kontrast sonrası T1 ağırlıklı görüntüler: Bu sekans özellikle herhangi bir enflamatuar sürecin veya vasküler anomalinin tespitini sağladığı için değerlidir. Gadolinyum kontrast maddesi, aktif lezyonlarla ilişkili artmış damarlanmayı göstererek aktif otosklerotik hastalık alanlarını da gösterebilir.
- 3D-FLAIR (Fluid-Attenuated Inversion Recovery) ve CISS (Constructive Interference in Steady State) sekansları: Bu sekanslar ise özellikle koklear implantasyon düşünülen vakalarda ameliyat öncesi değerlendirme için yararlı olan iç kulak yapılarının, koklear sinirin ayrıntılı görüntülerini sağlar.

3.2.2.1. MR Görüntüleme Bulguları

- Koklear Otoskleroz (Retrofenestral Otoskleroz): MRG, koklear tutulumun boyutunu değerlendirmede özellikle yararlıdır. T1 ağırlıklı görüntülerde hipointens alanlar ve T2 ağırlıklı görüntülerde hiperintens alanlar kemik

mineral içeriğinde ve ilik boşluklarında değişiklikler olduğunu gösterir. Kontrast sonrası perilabirentin/perikoklear bölgelerde sinyal artışları ise aktif enflamatuar süreçleri veya koklea içinde artmış vaskülariteyi gösterebilir.

- Retrokoklear Patolojilerin Ekartasyonu: MRG, vestibüler schwannoma veya otosklerozun bazı semptomlarını taklit edebilen diğer kraniyal sinir patolojileri gibi sensörinöral işitme kaybının diğer nedenlerini dışlamak için gereklidir.
- Koklear Açıklığın Değerlendirilmesi: Koklear implant planlaması için çok önemli olan koklea açıklığı kontrastlı MRG ile değerlendirilebilir.

Bu kısımda MRG'nin otoskleroz bağlamındaki uygulamalarını, özellikle de kokleanın değerlendirilmesindeki ve otosklerozun diğer iç kulak patolojilerinden ayırt edilmesindeki faydasını gösteren özet bilgiler aktarılmaya çalışılmıştır (Mangia ve ark., 2020; Goh ve ark., 2002; Ziyeh ve ark.1997; Purohit ve ark. 2020).

Sonuç olarak yüksek çözünürlüklü BT taraması başta olmak üzere radyolojik değerlendirme, otosklerozun kapsamlı bir şekilde değerlendirilmesinde çok önemli bir rol oynar. Tanının doğrulanmasına, hastalığın boyutunun anlaşılmasına ve cerrahi planlamanın kolaylaştırılmasına yardımcı olur. MRG'nin otoskleroz bağlamındaki uygulamalarını, özellikle de kokleanın değerlendirilmesindeki ve otosklerozun diğer iç kulak patolojilerinden ayırt edilmesindeki faydası bilinmektedir. Otosklerozda özellikle karmaşık vakalarda ve alternatif tanılar düşünüldüğünde görüntüleme vazgeçilmezdir ve BT ile MRG birbirini tamamlayıcı bilgiler sağlaması açısından değerlidir.

3.2.3. Görüntülemede Güncel Gelişmeler

3D-FLAIR MRG, otosklerozda koklear hasarın anlaşılmasına yardımcı olabilir ve tedavinin etkinliğinin izlenmesine ve tedavi için hastaların seçilmesine yardımcı olabilir Berrettini ve ark., 2018).

Son yıllarda FLAIR MRG'nin otosklerozda endolenfatik hidrops ve kan-labirent bariyerindeki bozulmayı değerlendirmek için kullanılabileceği bildirilmiştir (Laine ve ark., 2020).

AlexNet, VGGNet, GoogLeNet ve ResNet gibi derin öğrenme tekniklerinin, temporal kemik BT görüntülerinde otoskleroz tanısının konulmasında deneyimli radyologlara göre daha iyi sonuçlar vermesi açısından faydalı olabileceğini bildiren çalışmalar mevcuttur (Fujima ve ark, 2021).

4. AYIRICI TANI

Otoskleroz ayırıcı tanısında iletim tipi işitme kaybının diğer nedenlerini dışlamak çok önemlidir. Bunlar arasında kemikçik zincirde devamsızlıklar, timpanik membran perforasyonları ve diğer orta kulak patolojileri yer alır. Otosklerozu diğer orta ve iç kulak hastalıklarından sadece görüntüleme ile ayırt etmek, klinik ve odyometrik verilerle korelasyon olmadan zor olabilir. Saf ton odyometrisinde düşük ve yüksek frekansta hava-kemik boşluğundaki farklılıklar, statik kompliyans ve empedans odyometrisinde akustik refleks farklılıkları, klinik otosklerozu inküdostapedyal bağlantı kopmasından ayırmada faydalıdır (Kan ve ark., 2020).

Eş zamanlı otoskleroz ve superior semisirküler kanal dehisansının genellikle ayırt edilemeyen klinik tablolar olarak ortaya çıktığı ve stapedotominin genellikle kalıcı iletim tipi işitme kaybıyla sonuçlandığı ve hastaların %57-63'ünde semisirküler

kanal dehisansı semptomlarının maskelenmediği bildirilmiştir (Dewyer ve ark., 2019).

5. TEDAVİ

Otosklerozda tedavi işitmeyi iyileştirmeye odaklanır. Bu nedenle işitme cihazları kullanılabilir. Ya da fikse stapesin hareketliliği ve ses iletimi fonksiyonunu yeniden sağlamak için stapedektomi ve protez cerrahisi uygulanabilir. Fisch'in stapes ameliyatı tekniği, otoskleroz hastalarında hem hava yolu hem de kemik yolu eşiklerini iyileştirmektedir (Ren ve ark., 2018). Hastaların %87,2'sinde otosklerozun cerrahi tedavisi olarak stapedoplasti uygulandığını ve vakaların %87,2'sinde mükemmel sonuçlar elde edildiğini bildiren çalışma da mevcuttur (Gilifanov ve ark., 2018). Literatürde anormal kemik remodelingi engelleyerek/ilerlemesini yavaşlatarak durumu stabilize etmek için sodyum florür takviyesi ve bifosfonatın kullanılabileceği de belirtilmiştir (Jan ve ark., 2017; Zafar ve ark., 2024).

6. SONUÇ

Sonuç olarak otoskleroz tanısında hem klinik bulgular hem de başta yüksek çözünürlüklü BT taraması olmak üzere kapsamlı radyolojik değerlendirme çok önemlidir. Bu bakımdan hem klinisyenin hem de radyoloğun farkındalığı ve işbirliği içinde çalışması erken tanıyı sağlayabilir.

KAYNAKLAR

Abdelfatah, N., Mostafa, A. A., French, C. R., et al. (2022). A pathogenic deletion in Forkhead Box L1 (FOXL1) identifies the first otosclerosis (OTSC) gene. *Human genetics*, *141*(3-4), 965–979.

Anas, B., Sbai, A., Benlfadil, D., et al. (2023). Otosclerosis Surgery: Predictive Factors of Functional Results: 21 Cases. Scholars Journal of Medical Case Reports.

Berrettini, S., Lombardo, F., Bruschini, L., et al. (2018). 3D fluid attenuated inversion recovery (FLAIR) magnetic resonance imaging at different stages of otosclerosis. European Archives of Oto-Rhino-Laryngology, 275, 2643-2652.

Chen, W., Campbell, C., Green, G., et al. (2002). Linkage of otosclerosis to a third locus (OTSC3) on human chromosome 6p21.3-22.3. Journal of Medical Genetics, 39, 473 - 477.

Clarke-Brodber, A., & Taxy, J. (2021). The Stapes in Otosclerosis: Osteoarthritis of an Ear Ossicle. Head and Neck Pathology, 15, 737 - 742.

Crompton, M., Cadge, B., Ziff, J., et al. (2019). The Epidemiology of Otosclerosis in a British Cohort. Otology & neurotology: official publication of the American Otological Society, American Neurotology Society [and] European Academy of Otology and Neurotology, 40 1, 22-30 .

de Wit, C. A. D., van Dishoeck, H. A. E. (1964). Paracusis Willisii. *International Audiology*, *3*(1), 43–53.

Declau, F., Spaendonck, M., Timmermans, J., et al. (2001). Prevalence of Otosclerosis in an Unselected Series of Temporal Bones. Otology & Neurotology, 22, 596-602.

Dewyer, N., Quesnel, A., Santos, F. (2019). A Case Series of Patients With Concurrent Otosclerosis and Superior Semicircular Canal Dehiscence. Otology & Neurotology.

Doherty JK, Linthicum FH Jr. (2004). Spiral ligament and stria vascularis changes in cochlear otosclerosis: effect on hearing level. Otology & Neurotology: Official Publication of the American Otological Society, American Neurotology Society [and] European Academy of Otology and Neurotology. Jul;25(4):457-464.

Drabkin, M., Jean, M., Noy, Y., et al. (2023). SMARCA4 mutation causes human otosclerosis and a similar phenotype in mice. Journal of Medical Genetics.

Foster, M., & Backous, D. (2018). Clinical Evaluation of the Patient with Otosclerosis.. Otolaryngologic clinics of North America, 51 2, 319-326

Fujima, N., Andreu-Arasa, V., Onoue, K., et al. (2021). Utility of deep learning for the diagnosis of otosclerosis on temporal bone CT. European Radiology, 31, 5206 - 5211.

Gilifanov EA, Lepeiko BA, Andreeva LB, et al. (2018). [The diagnostics and surgical treatment of the patients presenting with otosclerosis in the Primorye Territory]. Vestnik Otorinolaringologii.;83(3):25-28.

Goh, J. P., Chan, L. L., & Tan, T. Y. (2002). MRI of cochlear otosclerosis. *The British journal of radiology*, *75*(894), 502–505.

Hansen, L., Bloch, S., & Sørensen, M. (2023). Cellular voids in the pathogenesis of otosclerosis. Acta Oto-Laryngologica, 143, 250 - 253.

House JW, Cunningham CD. Otosclerosis. In: Flint PW, et al (ed.) (2010). Cummings Otolaryngology Head and Neck Surgery, 5. ed. Philedelphia: Mosby-Elsevier;2028–35.

Jan, T. A., Remenschneider, A. K., Halpin, C., et al. (2017). Third-generation bisphosphonates for cochlear otosclerosis stabilizes sensorineural hearing loss in long-term follow-up. *Laryngoscope investigative otolaryngology*, *2*(5), 262–268.

Kan, T., Ueda, H., Kishimoto, M., et al. (2020). Availability of audiological evaluation for the differential diagnosis of clinical otosclerosis. Auris, nasus, larynx.

Kösling, S., Plontke, S., Bartel, S. (2020). Imaging of otosclerosis Bildgebung der Otosklerose. RöFo - Fortschritte auf dem Gebiet der Röntgenstrahlen und der bildgebenden Verfahren, 192, 745 - 753.

Laine, J., Hautefort, C., Attyé, A., et al. (2020). MRI evaluation of the endolymphatic space in otosclerosis and correlation with clinical findings. Diagnostic and interventional imaging.

Mafee MF, Valvassori GE, Becker M. Imaging of the head and neck. George Thieme Verlag. (2004) ISBN:1588900096.

Mangia, L., Coelho, L., Carvalho, B., et al. (2020). Imaging Studies in Otosclerosis: An Up-to-date Comprehensive Review. International Archives of Otorhinolaryngology, 25, e318 - e327.

Marshall, A. H., Fanning, N., Symons, S., et al. (2005). Cochlear implantation in cochlear otosclerosis. *The Laryngoscope, 115*(10), 1728–1733.

McKenna, M. J., Kristiansen, A. G., Bartley, M. L., et al. (1998). Association of COL1A1 and otosclerosis: evidence for a shared genetic etiology with mild osteogenesis imperfecta. *The American journal of otology*, *19*(5), 604–610.

Merchant, S. N., & Rosowski, J. J. (2008). Conductive hearing loss caused by third-window lesions of the inner ear. *Otology & neurotology: official publication of the American Otological Society, American Neurotology Society [and] European Academy of Otology and Neurotology*, *29*(3), 282–289.

Naumann, I. C., Porcellini, B., Fisch, U. (2005). Otosclerosis: incidence of positive findings on high-resolution computed tomography and their correlation to audiological test data. *The Annals of otology, rhinology, and laryngology*, *114*(9), 709–716.

Priyadarshi, S., Hansdah, K., Singh, N., et al. (2022). The risks of RELN polymorphisms and its expression in the development of otosclerosis. *PloS one*, *17*(6), e0269558.

Puiggrós, I., Moreno, E., Dotú, C., et al. (2023). Diagnostic Efficacy of High-Resolution Computed Tomography Densitometry for Diagnosing Otosclerosis. Otology & Neurotology, 44, e697 - e701.

Purohit, B., Op de Beeck, K., Hermans, R. (2020). Role of MRI as first-line modality in the detection of previously undiagnosed otosclerosis: a single tertiary institute experience. *Insights into imaging*, *11*(1), 71.

Quesnel, A., Ishai, R., McKenna, M. (2018). Otosclerosis: Temporal Bone Pathology. Otolaryngologic clinics of North America, 512,291-303.

Rämö, J., Kiiskinen, T., Karjalainen, J., et al. (2020). Genome-wide Screen of Otosclerosis in Population Biobanks: 18 Loci and Shared Heritability with Skeletal Structure. medRxiv.

Ren, Y., Wang, K., & Zhang, J. Q. (2018). *Lin chuang er bi yan hou tou jing wai ke za zhi = Journal of clinical*

otorhinolaryngology, head, and neck surgery, *32*(3), 199–201.

Salomone R, Riskalla PE, Vicente Ade O, Boccalini MC, Chaves AG, Lopes R, Felin Filho GB. Pediatric otosclerosis: case report and literature review. Braz J Otorhinolaryngol. 2008 Mar-Apr;74(2):303-6.

Sanghan, N., Chansakul, T., Kozin, E., et al. (2018). Retrospective Review of Otic Capsule Contour and Thickness in Patients with Otosclerosis and Individuals with Normal Hearing on CT. American Journal of Neuroradiology, 39, 2350 - 2355.

Tavernier, L., Fransen, E., Valgaeren, H., et al. (2021). Genetics of otosclerosis: finally catching up with other complex traits?. Human Genetics, 141, 939 - 950.

Valvassori G. E. (1993). Imaging of otosclerosis. *Otolaryngologic clinics of North America*, *26*(3), 359–371.

Venurkar, S., Rahate, N., Saha, S., et al. (2021). Otosclerosis: Etiology and Prognostic Factors. Journal of Pharmaceutical Research International.

Vîrzob, C., Closca, R., Poenaru, M., et al. (2023). Otosclerosis under the magnifying glass. Romanian Journal of Morphology and Embryology, 64, 189 - 197.

Wichova, H., Alvi, S., Boatright, C., et al. (2019). High-Resolution Computed Tomography of the Inner Ear: Effect of Otosclerosis on Cochlear Aqueduct Dimensions. Annals of Otology, Rhinology & Laryngology, 128, 749 - 754.

Wolfovitz, A., & Luntz, M. (2018). Impact of Imaging in Management of Otosclerosis. Otolaryngologic clinics of North America, 51 2, 343-355.

Zafar, N., Hohman, M. H., & Khan, M. A. B. (2024). Otosclerosis. In *StatPearls*. StatPearls Publishing.

Ziyeh, S., Berlis, A., Ross, U. H., Reinhardt, M. J., & Schumacher, M. (1997). MRI of active otosclerosis. *Neuroradiology*, *39*(6), 453–457.

RADIOLOGICAL IMAGING METHODS IN PROSTATE CANCER

Onur BAŞDEMİRCİ[1]

1. INTRODUCTION

Prostate gland is biggest accessory gland within the male reproductive system, located adjacent to bladder outlet and surrounding proximal urethra. It's responsible for producing an alkaline fluid that makes up about 25% of the ejaculate. Embryologically, it originates from the Wolffian duct and urogenital sinus. The bladder base is located superiorly, the symphysis pubis anteriorly, the rectum posteriorly, the urogenital diaphragm inferiorly, and the levator ani muscle inferolaterally. A pseudocapsule of fibromuscular tissue surrounds prostate gland. The neurovascular structures coming to the prostate gland pass through the pseudocapsule at 5 and 7 o'clock positions in the posterolateral direction and reach the prostate gland (Lee, Akin-Olugbade, & Kirschenbaum, 2011). Primary lymphatic drainage is to obturator, sacral, and internal iliac lymph nodes (Ryan, McNicholas, & Eustace, 2011). To a lesser extent, drainage is also available to external iliac and para-aortic lymph nodes (Lee et al., 2011; Shah & Zhou, 2019). The average weight in adults can be up to approximately 40 grams (Standring, 2020) and 30 ml is considered the upper limit for volume in imaging (Sandhu et al., 2024).

The prostate gland consists of four parts: anterior fibromuscular stroma, transitional zone, central zone and

[1] Radiology Specialist, Karabük Training and Research Hospital, Department of Radiology, o.basdemirci@gmail.com, ORCID: 0000-0003-4833-7377

peripheral zone. Transitional zone, which is the part surrounding the urethra, constitutes approximately 5% of prostate and Benign Prostatic Hyperplasia (BPH) occurs within this area (Ryan et al., 2011). BPH is a non-cancerous hyperplasia of prostate tissue and a prevalent disease, especially among men over 50. In elderly patients, BPH constitutes a significant portion of the causes of bladder outlet obstruction in terms of frequency. Peripheral zone accounts for approximately 70% of prostate and is the part where prostate cancer is most commonly seen. (Ryan et al., 2011).

Prostate cancer is most prevalent malignancy among males in developed countries and second most prevalent in less developed countries (Bray et al., 2024). Clinically, these patients may exhibit lower urinary tract symptoms like nocturia and frequent urination, and in advanced cases, hematuria and back pain (due to bone metastasis). Rectal examination, measurement of prostate-specific antigen (PSA) levels and transrectal biopsy are among the diagnostic methods for prostate cancer. In the current clinical approach, the first step in diagnosis is rectal examination and measurement of PSA level (Andriole et al., 2005). If tumor is located in transition zone or is small in size, there will be cause decrease in the sensitivity of the rectal examination. PSA is most important marker used in early diagnosis and follow-up of prostate cancer. However, PSA level is not a specific test and may also increase for some non-cancerous reasons. In addition, normal PSA values also do not exclude prostate cancer. Since the tumor cannot be distinguished in most cases even in transrectal USG, more than 30% false negative rates are reported in blind biopsies (Abd et al., 2011). The primary goal of imaging in prostate cancer is detection of prostate cancer at early stage. Imaging is relevant in detection of lesions in cases with suspected cancer, determining the risk level, reducing false-negative rates in biopsies by localizing the lesion before biopsy, and thus early diagnosis of prostate cancer.

Additionally, imaging methods are used for also post-diagnostic staging.

2. IMAGING METHODS

2.1.Ultrasonography (US)

Ultrasonography is oldest and most frequently used imaging method for evaluating the prostate gland. Although it's a readily available and low-cost imaging method that provides real-time imaging, it has limited tissue contrast in distinguishing between malignant and benign tumors. It is also dependent on user experience and has low specificity, especially in inexperienced users. Ultrasonographic imaging can be performed in two ways: transabdominal and transrectal. Transabdominal US has a lower resolution compared to transrectal US (TRUS) in detecting focal lesions. Therefore, transabdominal US is generally used to evaluate prostate volume, bladder wall, and postvoid residual volume in patients who experience symptoms of lower urinary tract, such as in BPH patients (Figure 1, 2). Also in distinguishable cases, focal lesions of the prostate, calcifications, obvious extraprostatic extensions and regional lymphadenopathies (LAP), if any, can be evaluated (Figure 3, 4).

Figure 1. Ultrasound images of 30-year-old patient; 1A: normal bladder and prostate, 1B: prostatic urethra, 1C: seminal vesicle are observed.

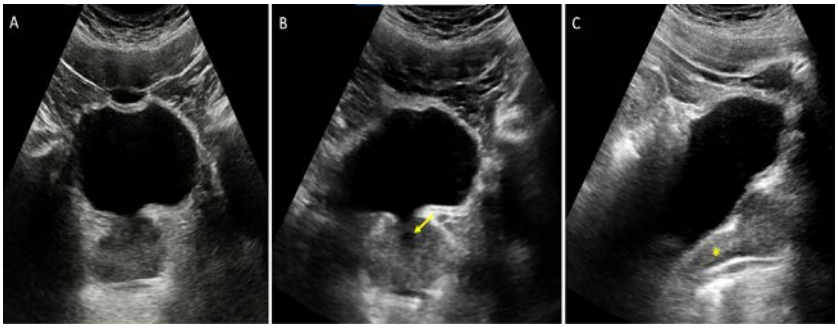

Figure 2. Ultrasound images of 54-year-old male patient under follow-up for BPH; 2A: increased prostate volume, 2B: prostatic indentation to bladder base, 2C: increased trabeculation of the bladder wall, 2D: millimetric hypoechoic nodular lesion in prostate gland is observed.

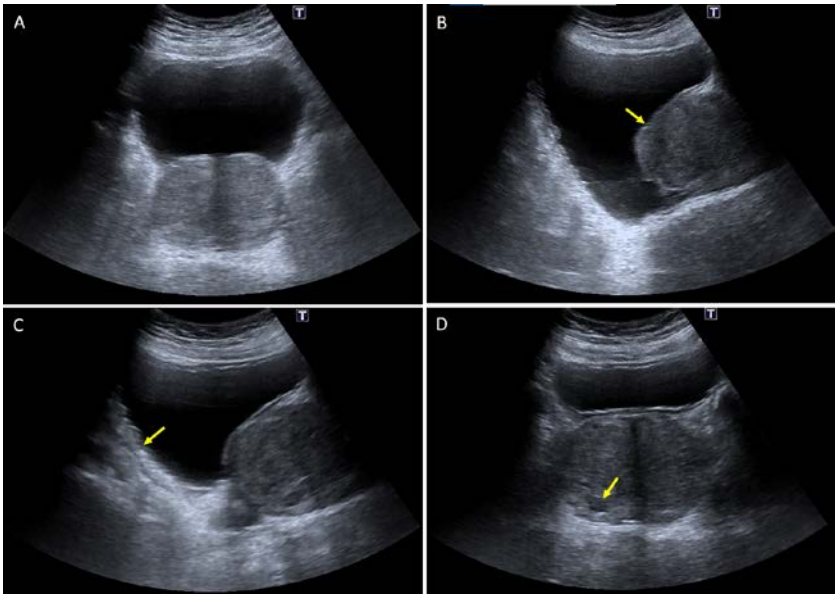

Figure 3. Ultrasound images of 52-year-old male patient; 3A: Transitional (TZ) and Peripheral (PZ) zones of prostate gland can be distinguished separately, 3B: hypodense nodular lesion in TZ are observed.

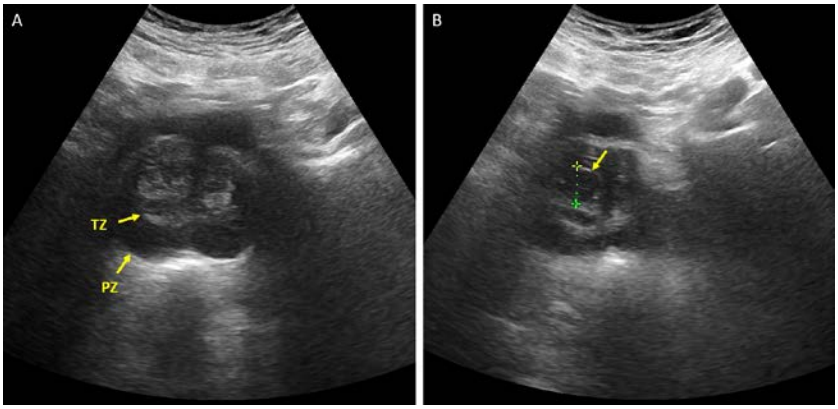

Figure 4. Ultrasound images of 46-year-old male patient; 4A: calcification with posterior acoustic shadowing in the prostate gland, 4B: twinkle artefact on Doppler ultrasound are observed.

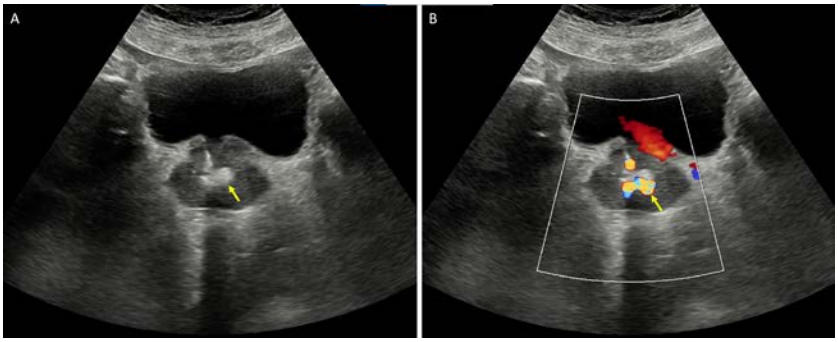

Although it has better resolution in detecting focal lesions compared to the transabdominal US, TRUS has a limited place in diagnosis and localization of prostate cancer. It's mostly used to direct and guide the biopsy. Although prostate cancers are generally not distinguished in standard US examinations, those that can be distinguished are usually observed as hypoechoic. However, they can also be seen as isoechoic or hyperechoic. Early-stage carcinomas may seen as isoechoic and it is thought that this condition is related to their relatively higher content of normal tissue (Ukimura, Faber, & Gill, 2012). Another limitation of standard B-mode ultrasonography is that also inflammatory conditions such as prostatitis and benign pathologies such as BPH can be observed hypoechoic. It has been reported in the literature that about 60% of biopsies performed on lesions that are suspicious in sonographic evaluation are benign (Loch et al., 2004) and about 21-47% of tumors can be skipped in the first biopsy (Taira et al., 2010). In addition, computer-aided evaluation techniques have been developed in TRUS, where the signal properties of B-mode images are processed in real time. Some studies in the literature are reporting that this computer-aided TRUS improves diagnostic performance compared to

conventional TRUS (Loch, 2007; Strunk, Decker, Willinek, Mueller, & Rogenhofer, 2014).

There are studies in the literature reporting that the US performed with sonographic contrast agents increases quality and more accurate results are obtained with fewer biopsies (Mitterberger et al., 2007). In TRUS performed with contrast material, malignant lesions can be seen as a rapid and asymmetric focal enhancement area due to neovascularization and angiogenesis occurring in the tumoral area (Postema, Mischi, de la Rosette, & Wijkstra, 2015). However, since there is no sonographic contrast agent in our country, contrast-enhanced US imaging cannot be performed in daily practice.

There are studies reporting that the use of elastography in addition to B mode US helps biopsy and has high sensitivity (Nelson, Slotoroff, Gomella, & Halpern, 2007). The elasticity and stiffness of prostate tissue can be evaluated using elastography. The increase in tissue stiffness in cancerous areas due to increased cellularity and deterioration in the glandular structure constitutes the basis of evaluation in US elastography. Areas with increased stiffness are considered more suspicious for malignancy (Pallwein et al., 2007). Several studies are reporting promising results, especially for shear wave elastography (Barr, Memo, & Schaub, 2012; Boehm et al., 2015; Correas et al., 2015). It has been stated that shear wave elastography has high applicability in prostate imaging; however, there is a decrease in reproducibility in the deep portions and lateral sections of the prostate gland. For this reason, it is recommended to be more careful in these areas when making US elastography assessment (Woo, Kim, Lee, Cho, & Kim, 2015).

One of the most important advantages of TRUS is that it guides biopsy. The disadvantages of blind biopsies are that prostate cancer can be multifocal, malignancy can be missed at

rates of up to 35% despite a negative biopsy result, and an increased number of biopsies can increase the risk of complications. Studies are ongoing to enable biopsy by localizing the lesion on the US rather than blind biopsy. For this purpose, some multiparametric US studies are being tested and developed by combining the various ultrasonography methods mentioned above (Aigner et al., 2012; Brock et al., 2012). Thus, in biopsies performed with TRUS, the aim is to increase diagnostic sensitivity-specificity, increase biopsy quality and decrease the number of unnecessary biopsies, thereby minimising risk of possible complications.

2.2.Magnetic Resonance Imaging (MRI)

MRI is effective imaging method that, because of its high contrast resolution, allows for differentiation of prostate gland's zonal anatomy and detection of any pathological signal changes in these regions (Hricak, Choyke, Eberhardt, Leibel, & Scardino, 2007). In prostate cancer, the primary indication of MRI is to evaluate extracapsular extension in patients diagnosed with cancer via biopsy (Hricak et al., 2007; Sala et al., 2006). MRI is increasingly being used clinically to detect and localize the tumor in cases where PSA levels remain elevated during follow-up but cancer is not detected in biopsies performed with TRUS.

In prostate imaging, the fundamental anatomical imaging sequence of MRI consists of high-resolution T2-weighted (T2W) sequences taken in three different planes. The addition of various functional imaging techniques to anatomical imaging has led to the concepts of biparametric and multiparametric MRI. Biparametric MRI is obtained by adding diffusion-weighted imaging (DWI) to T1W and T2W images. Multiparametric MRI, on the other hand, involves adding at least two functional techniques, like dynamic contrast-enhanced MRI, DWI, or MR spectroscopy, to T1W and T2W images. In a study including

1,140 patients, it was reported that the inclusion of mpMRI prior to biopsy guided by TRUS increased the likelihood of cancer detection from 38% to 72%. Additionally, in the same study, it was noted that none of the patients with a negative mpMRI had clinically significant cancer detected in the biopsies performed (Panebianco et al., 2015). A meta-analysis found that MRI-targeted biopsies enhance the detection rate of clinically significant cancers compared to systematic biopsies (from 76% to 91%). In addition, they reduce the detection rate of clinically insignificant cancers (from 83% to 44%) (Schoots et al., 2015).

Recommendations for sequence parameters in MRI are specified in PI-RADS v2.1 (Baris Turkbey et al., 2019). The non-contrast T1-weighted sequence is particularly used to evaluate the presence of bleeding in prostate and seminal vesicles, especially in patients with a history of prior biopsies (Figure 5). T2-weighted sequences, on the other hand, are one of the main sequences used to assess zonal anatomy of the prostate, signal changes in focal lesions, seminal vesicle invasion, and extraprostatic extension (Figure 6). Normal peripheral zone appears hyperintense on T2-weighted images due to high water content associated with its numerous ductal and acinar structures. In tumor tissue, there is a decrease in T2 signal due to increased cellularity. Therefore, while the edge characteristics of cancer tissue located in peripheral zone can vary, it's seen as a focal T2 hypointense area (Bhavsar & Verma, 2014). However, this appearance in T2-weighted images can also be seen in prostatitis, scar tissue, and hemorrhage, which ise making it not a specific finding for prostate cancer. In the transitional zone, higher smooth muscle content and lower glandular tissue result in the transitional zone appearing hypointense compared to the peripheral zone on T2-weighted images. Tumor tissue in the transitional zone is typically observed as a hypoechoic area with indistinct or spiculated contour features, often accompanied by signs of

invasion, and lacks a complete hypointense capsule around its periphery. Additionally, BPH nodules in the transitional zone can also appear hypointense, which complicates the differential diagnosis from cancer. In distinguishing between them, various features are evaluated, such as the presence or absence of a complete hypointense capsule in the periphery, signal homogeneity, and diffusion characteristics.

Figure 5. MRI images of a 64-year-old male patient; in left peripheral zone, hypointense on T2WI, hyperintense on T1WI, and a mildly diffusion-restricting hemorrhagic area are observed.

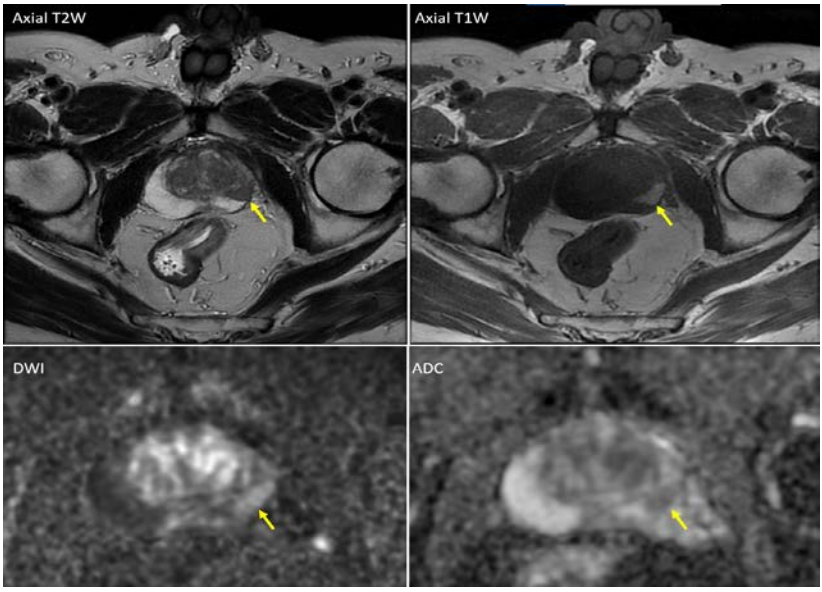

Figure 6. MRI images of 65-year-old male patient show a T2A hypointense, markedly diffusion-restricting PI-RADS 5 lesion extending to the transitional zone, invading the bilateral neurovascular bundle and seminal vesicle (arrows).

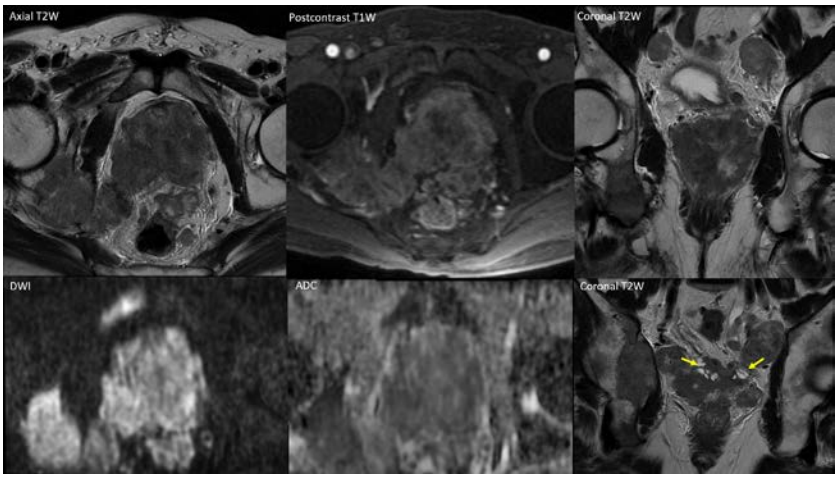

In prostate cancer, there is a decrease in extracellular volume due to increased cellularity, which subsequently restricts the free movement of water molecules (Brownian motion). This results in diffusion restriction, which is the basis for imaging in DWI (Russo, Mischi, Scheepens, De la Rosette, & Wijkstra, 2012). Images obtained with different magnetic field strengths are subtracted to create Apparent Diffusion Coefficient (ADC) maps. In ADC maps, prostate cancer typically shows lower ADC values, which correlate with the Gleason score of the lesion (Verma et al., 2011). An ADC value of less than 600 x 10-3 suggests the presence of a tumor, while a value greater than 1000 x 10-3 is more indicative of inflammation (Röthke, Blondin, Schlemmer, & Franiel, 2013) . DWI is also an effective method for detecting regional lymph nodes (Figure 7).

Figure 7. Multiple bone metastases (asterisks) and lymphadenopathy (arrows) are present in the MRI images of 65-year-old male patient, with regional lymphadenopathies more prominently observed in diffusion-weighted images.

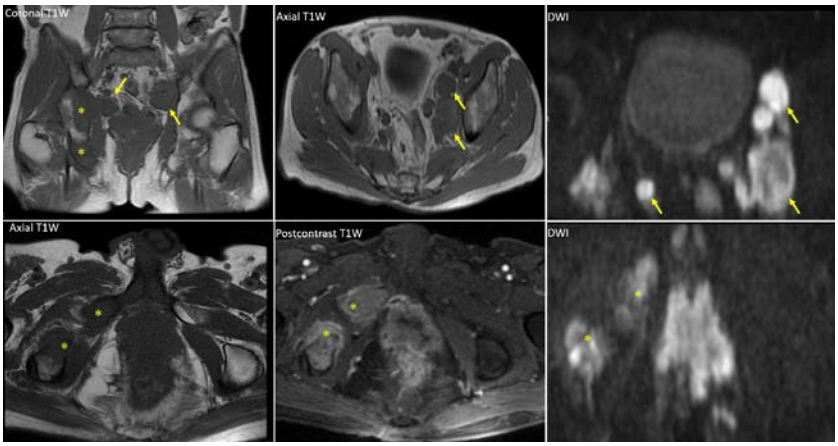

Dynamic contrast-enhanced MRI is obtained by acquiring T1-weighted images before and after the contrast agent administration. The increased angiogenesis in cancerous tissue results in the formation of vascular structures that have weaker and more permeable walls, leading to early and increased enhancement. As a result, prostate cancer manifests as a focal area of early enhancement in contrast-enhanced MRI. Additionally, the increased vascularity leads to higher blood flow and permeability, resulting in early wash-out. In summary, prostate cancer exhibits early enhancement, a higher peak, and early wash-out compared to normal prostate tissue (Röthke et al., 2013). This pattern of enhancement is more pronounced in high-grade tumors. However, in low-grade tumors, the lower levels of angiogenesis make it difficult to differentiate them with this technique (Ravizzini, Turkbey, Kurdziel, & Choyke, 2009).

MR spectroscopy (MRS) is an imaging technique that displays the levels of cellular metabolites. In normal prostate tissue, the citrate concentration is high. In tumor tissue, however,

there is an increase in choline levels, which serves as a marker for cell membrane turnover. In summary, prostate cancer is associated with a decrease in citrate levels and an increase in choline levels. MRS evaluation enhances the diagnostic sensitivity and specificity of multiparametric MRI (B. Turkbey et al., 2010). The acquisition of MRS images extends the duration of MRI scans and involves additional technical requirements, while their interpretation requires a certain level of expertise (Testa et al., 2007). For these reasons, in clinical practice, it is used more for evaluating treatment response and recurrence rather than for the initial diagnosis of prostate cancer.

To standardize the assessment and reporting of prostate MRI, the European Society of Urogenital Radiology published the Prostate Imaging Reporting and Data System (PI-RADS) guidelines for the first time in 2012 (Barentsz et al., 2012). A meta-analysis in the literature reported that the sensitivity of the first version was 0.78, the specificity was 0.79, and the negative predictive value varied between 0.58 and 0.95 (Hamoen, de Rooij, Witjes, Barentsz, & Rovers, 2015). However, following advancements in clinical and imaging fields, certain limitations were identified, leading to modifications and updates in the guidelines. As a result, PI-RADS V2 was published in 2014. In PI-RADS V2, the defining sequences for the transitional and peripheral zones and the steps to be followed for various scenarios are outlined. Updates were also made to the prostate sector map (Weinreb et al., 2016). Since the release of PI-RADS V2, it has been extensively utilized in clinical settings and research. Many studies in the literature have compared it to the previous version, examined its diagnostic effectiveness, and evaluated inter-observer consistency related to PI-RADS V2 (Purysko et al., 2017; Seo et al., 2017; Woo, Suh, Kim, Cho, & Kim, 2017). A meta-analysis reported that the sensitivity of PI-RADS V2 is 0.89 and its specificity is 0.73, indicating that its sensitivity is higher

compared to PI-RADS V1 (Woo et al., 2017). However, as a result of these studies, some limitations of PI-RADS V2 have become apparent over time. It has been reported that inter-observer agreement is moderate, and several evaluation criteria that need improvement and further clarification have been identified (Rosenkrantz, Ginocchio, et al., 2016; Rosenkrantz, Oto, Turkbey, & Westphalen, 2016). As a result, PI-RADS V2.1 was published in 2019. This version includes technical details, requirements, and standardizations related to the acquisition of sequences, as well as modifications in scoring for risk classification based on sector maps and zones (Baris Turkbey et al., 2019). The updated sector map includes a total of 41 sectors: 38 for the prostate, 2 for the seminal vesicles, and 1 for the membranous urethra.

PI-RADS v2 provides a definition for clinically significant cancer. Cancers with a Gleason score of 7 or higher, and/or a volume of 0.5 cc or greater, and/or extraprostatic extension are defined as clinically significant cancers (ACR, 2015). Besides establishing a common language and reporting standards, the main goal of the PI-RADS classification and scoring system isto predict the likelihood of clinically significant cancer with high sensitivity and specificity. In PI-RADS v2.1, each prostate lesion is scored on a scale from 1 to 5 for the likelihood of clinically significant cancer, based on the evaluation of T2A, DWI, and dynamic contrast-enhanced MRI images. Based on PI-RADS v2.1 the evaluation categories are:

PI-RADS category 1: Very low (Clinically significant cancer is very unlikely)

PI-RADS category 2: Low (Clinically significant cancer is probably absent)

PI-RADS category 3: Moderate (Clinically significant cancer is suspected)

PI-RADS category 4: High (Clinically significant cancer is probable)

PI-RADS category 5: Very high (Clinically significant cancer is highly probable)

The general approach recommends performing a biopsy for PI-RADS 4 and 5 lesions and not conducting one for PI-RADS 1 and 2 lesions. However, for PI-RADS 3 lesions, decisions are made based on MRI findings as well as the patient's clinical history, PSA levels, local preferences in patient management, expertise, and care standards. PI-RADS v2.1 does not include management recommendations; however, as evidence regarding mpMRI and MRI-targeted biopsies and interventions continues to accumulate, it is anticipated that specific recommendations and algorithms related to biopsy and management will be included in future versions of PI-RADS (PI-RADS: Prostate Imaging – Reporting and Data System. Version 2.1, 2019).

2.3.Computed Tomography (CT)

Although its role in detection of prostate cancer and local staging is limited, another radiological method used in newly diagnosed cases is computed tomography (CT). Because of CT's insufficient contrast resolution, the prostate zones cannot be distinctly identified, and it is also difficult to differentiate the prostate gland from the adjacent levator ani muscle, which has a similar density. For similar reasons, tumors within the prostate gland are often not accurately localized. However, it can be useful in lesions with significant vascularity or those exhibiting extraprostatic extension. Although its role in localization and local staging is limited, CT is a preferred and effective method in clinical practice for investigating regional lymphadenopathy, bone metastases, and distant organ metastases, as well as for follow-up after treatment (Vinjamoori et al., 2012). (Figure 8).

Thin-slice CT images are highly effective for imaging lymph nodes. However, a metastatic lymph node can appear normal in size, and lymph nodes can also enlarge due to reactive hyperplasia caused by non-metastatic factors like infection. For these reasons, the assessment of size and morphology using CT has limited effectiveness in differentiating metastatic from reactive lymph nodes, with a sensitivity reported at approximately 36% (Hricak et al., 2007). Bone metastases of prostate cancer may appear as either lytic or sclerotic lesions. The literature reports that sensitivity of CT for identifying bone metastases is 56%, with a specificity of 74% (O'Sullivan, Carty, & Cronin, 2015). In some cases, bone metastases may be indistinguishable on CT but can be differentiated using scintigraphy and PET. However, due to its greater accessibility and relatively lower cost, CT is recommended in the guidelines of American Urological Association for patients who have moderate-high risk for prostate cancer. (Ghafoor, Burger, & Vargas, 2019).

Figure 8. In the CT images of a 65-year-old male patient, multiple bone metastases (asterisks) and metastatic lung nodules (arrows) are observed.

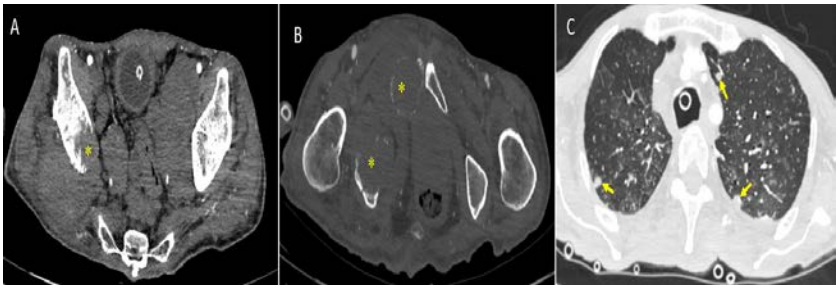

3. CONCLUSION

Imaging techniques are becoming increasingly important for the early recognition and management of prostate cancer, allowing for more accurate diagnoses due to advancements in imaging technology.

REFERENCES

Abd, T. T., Goodman, M., Hall, J., Ritenour, C. W., Petros, J. A., Marshall, F. F., & Issa, M. M. (2011). Comparison of 12-core versus 8-core prostate biopsy: multivariate analysis of large series of US veterans. Urology, 77(3), 541-547. doi:10.1016/j.urology.2010.06.008

ACR. (2015). Prostate Imaging and Reporting and Data System: Version 2. In.

Aigner, F., Schäfer, G., Steiner, E., Jaschke, W., Horninger, W., Herrmann, T. R., . . . Frauscher, F. (2012). Value of enhanced transrectal ultrasound targeted biopsy for prostate cancer diagnosis: a retrospective data analysis. World J Urol, 30(3), 341-346. doi:10.1007/s00345-011-0809-6

Andriole, G. L., Levin, D. L., Crawford, E. D., Gelmann, E. P., Pinsky, P. F., Chia, D., . . . Gohagan, J. K. (2005). Prostate Cancer Screening in the Prostate, Lung, Colorectal and Ovarian (PLCO) Cancer Screening Trial: findings from the initial screening round of a randomized trial. J Natl Cancer Inst, 97(6), 433-438. doi:10.1093/jnci/dji065

Barentsz, J. O., Richenberg, J., Clements, R., Choyke, P., Verma, S., Villeirs, G., . . . Fütterer, J. J. (2012). ESUR prostate MR guidelines 2012. Eur Radiol, 22(4), 746-757. doi:10.1007/s00330-011-2377-y

Barr, R. G., Memo, R., & Schaub, C. R. (2012). Shear wave ultrasound elastography of the prostate: initial results. Ultrasound Q, 28(1), 13-20. doi:10.1097/RUQ.0b013e318249f594

Bhavsar, A., & Verma, S. (2014). Anatomic imaging of the prostate. Biomed Res Int, 2014, 728539. doi:10.1155/2014/728539

Boehm, K., Salomon, G., Beyer, B., Schiffmann, J., Simonis, K., Graefen, M., & Budaeus, L. (2015). Shear wave elastography for localization of prostate cancer lesions and assessment of elasticity thresholds: implications for targeted biopsies and active surveillance protocols. J Urol, 193(3), 794-800. doi:10.1016/j.juro.2014.09.100

Bray, F., Laversanne, M., Sung, H., Ferlay, J., Siegel, R. L., Soerjomataram, I., & Jemal, A. (2024). Global cancer statistics 2022: GLOBOCAN estimates of incidence and mortality worldwide for 36 cancers in 185 countries. CA Cancer J Clin, 74(3), 229-263. doi:10.3322/caac.21834

Brock, M., von Bodman, C., Palisaar, R. J., Löppenberg, B., Sommerer, F., Deix, T., . . . Eggert, T. (2012). The impact of real-time elastography guiding a systematic prostate biopsy to improve cancer detection rate: a prospective study of 353 patients. J Urol, 187(6), 2039-2043. doi:10.1016/j.juro.2012.01.063

Correas, J. M., Tissier, A. M., Khairoune, A., Vassiliu, V., Méjean, A., Hélénon, O., . . . Barr, R. G. (2015). Prostate cancer: diagnostic performance of real-time shear-wave elastography. Radiology, 275(1), 280-289. doi:10.1148/radiol.14140567

Ghafoor, S., Burger, I. A., & Vargas, A. H. (2019). Multimodality Imaging of Prostate Cancer. J Nucl Med, 60(10), 1350-1358. doi:10.2967/jnumed.119.228320

Hamoen, E. H. J., de Rooij, M., Witjes, J. A., Barentsz, J. O., & Rovers, M. M. (2015). Use of the Prostate Imaging Reporting and Data System (PI-RADS) for Prostate Cancer Detection with Multiparametric Magnetic Resonance Imaging: A Diagnostic Meta-analysis. Eur Urol, 67(6), 1112-1121. doi:10.1016/j.eururo.2014.10.033

Hricak, H., Choyke, P. L., Eberhardt, S. C., Leibel, S. A., & Scardino, P. T. (2007). Imaging prostate cancer: a multidisciplinary perspective. Radiology, 243(1), 28-53. doi:10.1148/radiol.2431030580

Lee, C. H., Akin-Olugbade, O., & Kirschenbaum, A. (2011). Overview of prostate anatomy, histology, and pathology. Endocrinol Metab Clin North Am, 40(3), 565-575, viii-ix. doi:10.1016/j.ecl.2011.05.012

Loch, T. (2007). Computerized transrectal ultrasound (C-TRUS) of the prostate: detection of cancer in patients with multiple negative systematic random biopsies. World J Urol, 25(4), 375-380. doi:10.1007/s00345-007-0181-8

Loch, T., Eppelmann, U., Lehmann, J., Wullich, B., Loch, A., & Stöckle, M. (2004). Transrectal ultrasound guided biopsy of the prostate: random sextant versus biopsies of sono-morphologically suspicious lesions. World J Urol, 22(5), 357-360. doi:10.1007/s00345-004-0462-4

Mitterberger, M., Horninger, W., Pelzer, A., Strasser, H., Bartsch, G., Moser, P., . . . Frauscher, F. (2007). A prospective randomized trial comparing contrast-enhanced targeted versus systematic ultrasound guided biopsies: impact on prostate cancer detection. Prostate, 67(14), 1537-1542. doi:10.1002/pros.20639

Nelson, E. D., Slotoroff, C. B., Gomella, L. G., & Halpern, E. J. (2007). Targeted biopsy of the prostate: the impact of color Doppler imaging and elastography on prostate cancer detection and Gleason score. Urology, 70(6), 1136-1140. doi:10.1016/j.urology.2007.07.067

O'Sullivan, G. J., Carty, F. L., & Cronin, C. G. (2015). Imaging of bone metastasis: An update. World J Radiol, 7(8), 202-211. doi:10.4329/wjr.v7.i8.202

Pallwein, L., Mitterberger, M., Struve, P., Pinggera, G., Horninger, W., Bartsch, G., . . . Frauscher, F. (2007). Real-time elastography for detecting prostate cancer: preliminary experience. BJU Int, 100(1), 42-46. doi:10.1111/j.1464-410X.2007.06851.x

Panebianco, V., Barchetti, F., Sciarra, A., Ciardi, A., Indino, E. L., Papalia, R., . . . Catalano, C. (2015). Multiparametric magnetic resonance imaging vs. standard care in men being evaluated for prostate cancer: a randomized study. Urol Oncol, 33(1), 17.e11-17.e17. doi:10.1016/j.urolonc.2014.09.013

PI-RADS: Prostate Imaging – Reporting and Data System. Version 2.1. (2019). In.

Postema, A., Mischi, M., de la Rosette, J., & Wijkstra, H. (2015). Multiparametric ultrasound in the detection of prostate cancer: a systematic review. World J Urol, 33(11), 1651-1659. doi:10.1007/s00345-015-1523-6

Purysko, A. S., Bittencourt, L. K., Bullen, J. A., Mostardeiro, T. R., Herts, B. R., & Klein, E. A. (2017). Accuracy and Interobserver Agreement for Prostate Imaging Reporting and Data System, Version 2, for the Characterization of Lesions Identified on Multiparametric MRI of the Prostate. AJR Am J Roentgenol, 209(2), 339-349. doi:10.2214/ajr.16.17289

Ravizzini, G., Turkbey, B., Kurdziel, K., & Choyke, P. L. (2009). New horizons in prostate cancer imaging. Eur J Radiol, 70(2), 212-226. doi:10.1016/j.ejrad.2008.09.019

Rosenkrantz, A. B., Ginocchio, L. A., Cornfeld, D., Froemming, A. T., Gupta, R. T., Turkbey, B., . . . Margolis, D. J. (2016). Interobserver Reproducibility of the PI-RADS Version 2 Lexicon: A Multicenter Study of Six

Experienced Prostate Radiologists. Radiology, 280(3), 793-804. doi:10.1148/radiol.2016152542

Rosenkrantz, A. B., Oto, A., Turkbey, B., & Westphalen, A. C. (2016). Prostate Imaging Reporting and Data System (PI-RADS), Version 2: A Critical Look. AJR Am J Roentgenol, 206(6), 1179-1183. doi:10.2214/ajr.15.15765

Röthke, M., Blondin, D., Schlemmer, H. P., & Franiel, T. (2013). [PI-RADS classification: structured reporting for MRI of the prostate]. Rofo, 185(3), 253-261. doi:10.1055/s-0032-1330270

Russo, G., Mischi, M., Scheepens, W., De la Rosette, J. J., & Wijkstra, H. (2012). Angiogenesis in prostate cancer: onset, progression and imaging. BJU Int, 110(11 Pt C), E794-808. doi:10.1111/j.1464-410X.2012.11444.x

Ryan, S., McNicholas, M., & Eustace, S. J. (2011). Anatomy for Diagnostic Imaging: Saunders/Elsevier.

Sala, E., Eberhardt, S. C., Akin, O., Moskowitz, C. S., Onyebuchi, C. N., Kuroiwa, K., . . . Hricak, H. (2006). Endorectal MR imaging before salvage prostatectomy: tumor localization and staging. Radiology, 238(1), 176-183. doi:10.1148/radiol.2381052345

Sandhu, J. S., Bixler, B. R., Dahm, P., Goueli, R., Kirkby, E., Stoffel, J. T., & Wilt, T. J. (2024). Management of Lower Urinary Tract Symptoms Attributed to Benign Prostatic Hyperplasia (BPH): AUA Guideline Amendment 2023. J Urol, 211(1), 11-19. doi:10.1097/ju.0000000000003698

Schoots, I. G., Roobol, M. J., Nieboer, D., Bangma, C. H., Steyerberg, E. W., & Hunink, M. G. (2015). Magnetic resonance imaging-targeted biopsy may enhance the diagnostic accuracy of significant prostate cancer

detection compared to standard transrectal ultrasound-guided biopsy: a systematic review and meta-analysis. Eur Urol, 68(3), 438-450. doi:10.1016/j.eururo.2014.11.037

Seo, J. W., Shin, S. J., Taik Oh, Y., Jung, D. C., Cho, N. H., Choi, Y. D., & Park, S. Y. (2017). PI-RADS Version 2: Detection of Clinically Significant Cancer in Patients With Biopsy Gleason Score 6 Prostate Cancer. AJR Am J Roentgenol, 209(1), W1-w9. doi:10.2214/ajr.16.16981

Shah, R. B., & Zhou, M. (2019). Prostate Biopsy Interpretation: An Illustrated Guide: Springer International Publishing.

Standring, S. (2020). Gray's Anatomy: The Anatomical Basis of Clinical Practice: Elsevier.

Strunk, T., Decker, G., Willinek, W., Mueller, S. C., & Rogenhofer, S. (2014). Combination of C-TRUS with multiparametric MRI: potential for improving detection of prostate cancer. World J Urol, 32(2), 335-339. doi:10.1007/s00345-012-0924-z

Taira, A. V., Merrick, G. S., Galbreath, R. W., Andreini, H., Taubenslag, W., Curtis, R., . . . Wallner, K. E. (2010). Performance of transperineal template-guided mapping biopsy in detecting prostate cancer in the initial and repeat biopsy setting. Prostate Cancer Prostatic Dis, 13(1), 71-77. doi:10.1038/pcan.2009.42

Testa, C., Schiavina, R., Lodi, R., Salizzoni, E., Corti, B., Farsad, M., . . . Barbiroli, B. (2007). Prostate cancer: sextant localization with MR imaging, MR spectroscopy, and 11C-choline PET/CT. Radiology, 244(3), 797-806. doi:10.1148/radiol.2443061063

Turkbey, B., Pinto, P. A., Mani, H., Bernardo, M., Pang, Y., McKinney, Y. L., . . . Choyke, P. L. (2010). Prostate cancer: value of multiparametric MR imaging at 3 T for

detection--histopathologic correlation. Radiology, 255(1), 89-99. doi:10.1148/radiol.09090475

Turkbey, B., Rosenkrantz, A. B., Haider, M. A., Padhani, A. R., Villeirs, G., Macura, K. J., . . . Weinreb, J. C. (2019). Prostate Imaging Reporting and Data System Version 2.1: 2019 Update of Prostate Imaging Reporting and Data System Version 2. Eur Urol, 76(3), 340-351. doi:https://doi.org/10.1016/j.eururo.2019.02.033

Ukimura, O., Faber, K., & Gill, I. S. (2012). Intraprostatic targeting. Curr Opin Urol, 22(2), 97-103. doi:10.1097/MOU.0b013e32835017fa

Verma, S., Rajesh, A., Morales, H., Lemen, L., Bills, G., Delworth, M., . . . Lamba, M. (2011). Assessment of aggressiveness of prostate cancer: correlation of apparent diffusion coefficient with histologic grade after radical prostatectomy. AJR Am J Roentgenol, 196(2), 374-381. doi:10.2214/ajr.10.4441

Vinjamoori, A. H., Jagannathan, J. P., Shinagare, A. B., Taplin, M. E., Oh, W. K., Van den Abbeele, A. D., & Ramaiya, N. H. (2012). Atypical metastases from prostate cancer: 10-year experience at a single institution. AJR Am J Roentgenol, 199(2), 367-372. doi:10.2214/ajr.11.7533

Weinreb, J. C., Barentsz, J. O., Choyke, P. L., Cornud, F., Haider, M. A., Macura, K. J., . . . Verma, S. (2016). PI-RADS Prostate Imaging - Reporting and Data System: 2015, Version 2. Eur Urol, 69(1), 16-40. doi:10.1016/j.eururo.2015.08.052

Woo, S., Kim, S. Y., Lee, M. S., Cho, J. Y., & Kim, S. H. (2015). Shear wave elastography assessment in the prostate: an intraobserver reproducibility study. Clin Imaging, 39(3), 484-487. doi:10.1016/j.clinimag.2014.11.013

Woo, S., Suh, C. H., Kim, S. Y., Cho, J. Y., & Kim, S. H. (2017). Diagnostic Performance of Prostate Imaging Reporting and Data System Version 2 for Detection of Prostate Cancer: A Systematic Review and Diagnostic Meta-analysis. Eur Urol, 72(2), 177-188. doi:10.1016/j.eururo.2017.01.042

RADYOLOJİ

yaz
yayınları

YAZ Yayınları
M.İhtisas OSB Mah. 4A Cad. No:3/3
İscehisar / AFYONKARAHİSAR
Tel : (0 531) 880 92 99
yazyayinlari@gmail.com • www.yazyayinlari.com